HHS Public Access

Author manuscript

J Immunol. Author manuscript; available in PMC 2018 April 01.

Published in final edited form as:

J Immunol. 2017 April 01; 198(7): 2943–2956. doi:10.4049/jimmunol.1601639.

Immature Lymphocytes Inhibit *Rag1* and *Rag2* Transcription and V(D)J Recombination in Response to DNA Double Strand Breaks

Megan R. Fisher[*,†,‡], **Adrian Rivera-Reyes**[*,‡,§], **Noah B. Bloch**[*], **David G. Schatz**[¶], and **Craig H. Bassing**[*,†,‡,§,‖]

[*]Division of Cancer Pathobiology, Department of Pathology and Laboratory Medicine, Center for Childhood Cancer Research, Children's Hospital of Philadelphia, Philadelphia, PA 19104

[†]Immunology Graduate Group, Perelman School of Medicine at the University of Pennsylvania, Philadelphia, PA 19104

[‡]Department of Pathology and Laboratory Medicine, Abramson Family Cancer Research Institute, Perelman School of Medicine at the University of Pennsylvania, Philadelphia, PA 19104

[§]Cancer Biology Program of the Cell and Molecular Biology Graduate Group, Perelman School of Medicine at the University of Pennsylvania, Philadelphia, PA 19104

[¶]Department of Immunobiology, Yale University School of Medicine, Howard Hughes Medical Institute, 300 Cedar Street, Box 208011, New Haven, CT 06520

Abstract

Mammalian cells have evolved a common DNA damage response (DDR) that sustains cellular function, maintains genomic integrity, and suppresses malignant transformation. In pre-B cells, DNA double strand breaks (DSBs) induced at *Igκ* loci by the Rag1/Rag2 (RAG) endonuclease engage this DDR to modulate transcription of genes that regulate lymphocyte-specific processes. We previously reported that RAG DSBs induced at one *Igκ* allele signal through the ATM kinase to feedback inhibit RAG expression and RAG cleavage of the other *Igκ* allele. Here, we show that DSBs induced by ionizing radiation, etoposide, or bleomycin suppress Rag1 and Rag2 mRNA levels in primary pre-B cells, pro-B cells, and pro-T cells, indicating that inhibition of *Rag1* and *Rag2* expression is a prevalent DSB response among immature lymphocytes. DSBs induced in pre-B cells signal rapid transcriptional repression of *Rag1* and *Rag2*, causing downregulation of both Rag1 and Rag2 mRNA but only Rag1 protein. This transcriptional inhibition requires the ATM kinase and the NF-κB essential modulator protein, implicating a role for ATM-mediated activation of canonical NF-κB transcription factors. Finally, we demonstrate that DSBs induced in pre-B cells by etoposide or bleomycin inhibit recombination of *Igκ* loci and a chromosomally integrated substrate. Our data indicate that immature lymphocytes exploit a common DDR signaling pathway to limit DSBs at multiple genomic locations within developmental stages wherein monoallelic antigen receptor locus recombination is enforced. We discuss the implications

[‖]Corresponding Author: Craig H. Bassing, Ph.D., Children's Hospital of Philadelphia, 4054 Colket Translational Research Building, 3501 Civic Center Blvd., Philadelphia, PA 19104, Phone: 267-426-0311, FAX: 267-426-2791, bassing@email.chop.edu.

C.H.B. is a consultant for Regeneron Pharmaceuticals. None of the other authors have potential conflicts of interest.

of our findings for mechanisms that orchestrate the differentiation of mono-specific lymphocytes while suppressing oncogenic antigen receptor locus translocations.

Introduction

DSBs are unavoidable, common, and hazardous genomic lesions. They are induced by endogenous factors including cellular metabolites, gene transcription, and DNA replication, and by exogenous factors including ionizing radiation (IR) and genotoxic drugs. DSBs can impair cellular function, induce apoptosis, or create genomic alterations that cause cancer if they are not repaired or are aberrantly repaired. Mammalian cells have evolved a conserved DDR that coordinates DSB repair with cellular proliferation and survival to maintain cellular function, preserve genomic integrity, and suppress malignant transformation. A central component of this shared DDR is the Ataxia Telangiectasia mutated (ATM) kinase, which is activated by DSBs (1). ATM phosphorylates and activates DNA repair proteins to enhance the kinetics and fidelity of DSB repair (2). ATM also activates intracellular signaling pathways that maintain cellular survival and halt DNA synthesis as cells attempt to repair DSBs, and promote apoptosis if DSBs are not repaired (1). For example, ATM phosphorylates the NF-κB essential modulator (Nemo) protein to activate NF-κB-mediated transcription of anti-apoptotic genes (3). In parallel, ATM-dependent phosphorylation of the Tp53 protein activates transcription of cell cycle checkpoint and pro-apoptotic genes (1). The importance of the conserved mammalian DDR is highlighted by the increased predisposition of humans and mice lacking ATM protein to oncogenic genomic instability (4–8).

Despite their inherent danger, DSBs are essential for mammalian biology. The programmed induction of DSBs by tissue-specific proteins is necessary to establish the genetic diversity that drives evolution and provides adaptive immunity (9, 10). A paradigm for this concept is the assembly of Ag receptor (AgR) gene variable region exons via recombination of variable (V), diversity (D), and joining (J) gene segments in developing B and T cells (11). The lymphocyte-specific RAG endonuclease catalyzes V(D)J recombination in G1 phase cells by cleaving at recombination signal sequences (RSSs) that flank all V, D, and J segments (12). The resolution of RAG DSBs by non-homologous end-joining (NHEJ) factors generates V(D)J coding joins and RSS signal joins (2). These V(D)J exons and downstream constant region exons comprise assembled AgR genes. The large number of possible V(D)J joining events and the inherent imprecision of coding join formation cooperate to establish AgR gene diversity. The essential role for RAG DSBs in establishing immunity is emphasized by mutations of RAG1, RAG2, RSSs, or NHEJ factors that impair lymphocyte development, restrict AgR gene repertoires, and cause fatal severe combined immunodeficiency (13–15).

RAG DSBs and the DDR cooperate to promote and police AgR gene assembly and differentiation of lymphocytes in the bone marrow (B lymphocytes) and thymus (T lymphocytes). The assembly of IgH or TCRβ genes in pro-B or pro-T cells, respectively, generates pre-BCR or pre-TCR complexes that signal cellular proliferation and differentiation into pre-B or pre-T cells (16). Similarly, assembly of IgL (Igκ or Igλ) or TCRα genes in pre-B or pre-T cells, respectively, forms BCR and αβ TCR AgRs that signal

cellular differentiation or apoptosis (16). Autoreactive AgRs induce receptor editing through further IgL recombination or apoptosis; while innocuous AgRs halt *Rag1* and *Rag2* transcription and drive differentiation of conventional B and αβ T cells (17). In pro-T cells, the assembly of TCRγ and TCRδ genes also occurs and when successful produces γδ TCRs that terminate *Rag1* and *Rag2* transcription and signal differentiation of γδ T cells (18). RAG cleavage of AgR loci activates the ATM kinase (19), which phosphorylates DSB repair proteins to prevent degradation and enhance joining of RAG-liberated DNA ends (2). ATM also activates Tp53 to trigger the G1/S cell cycle checkpoint, inhibiting cells with RAG DSBs from entering S phase where DNA replication-associated DSBs increase the probability for AgR locus translocations (20, 21) At least in pre-B cells, RAG DSBs signal through both ATM-dependent and ATM-independent pathways to activate a broad multifunctional genetic program that includes genes known to regulate lymphocyte differentiation and lymphocyte-specific processes (22). One of these pathways involves ATM-dependent Nemo phosphorylation, which induces NF-κB-mediated transcription of the anti-apoptotic *Pim2* gene to prolong the survival of pre-B cells recombining IgL genes (22, 23).

Recent work from our lab and the Sleckman lab has revealed that lymphocyte-specific RAG DSBs cooperate with common DDR signaling pathways to transiently feedback inhibit AgR gene assembly. We demonstrated that RAG cleavage of one *Igκ* allele in primary pre-B cells signals via the ATM kinase to suppress RAG cleavage of the other allele (24). ATM also downregulates the levels of Rag1 and Rag2 mRNA and Rag1 protein, as well as mRNA and protein levels of Gadd45α (24), which had been shown to signal *Rag1* and *Rag2* transcription in a pre-B cell line (25). However, the asynchronous induction of RAG DSBs at *Igκ* alleles precluded investigating the kinetics or mechanism of RAG downregulation or a potential mechanistic link between suppression of Gadd45α protein and repression of Rag1 and Rag2 mRNA. We proposed that RAG DSB-induced feedback inhibition of RAG expression limits simultaneous RAG cleavage of distinct AgR alleles, helping to enforce mono-allelic assembly and expression (allelic exclusion) of Igκ, IgH, and TCRβ genes and to suppress oncogenic IgH, TCRβ, and TCRδ translocations during proliferation of pro-B and pro-T cells (24, 26). Consistent with this idea, we showed that mice lacking ATM develop higher than normal frequencies of lymphocytes with bi-allelic expression and/or translocations of Igκ, IgH, or TCRβ loci (26). The Sleckman lab found that RAG DSBs induced at one Igκ allele signal via ATM to activate expression of the hematopoietic-specific SpiC transcriptional repressor (27). SpiC inhibits RAG cleavage of the other *Igκ* allele by suppressing transcription-linked accessibility of Jκ gene segments to the RAG endonuclease (27). This body of work established the concept of DSB-induced feedback inhibition of Igκ recombination by RAG cleavage and demonstrated that this regulation involves ATM-dependent DDR signaling pathways that repress RAG expression and *Igκ* recombination potential.

Since DSBs induced in pre-B cells by ionizing radiation or etoposide can activate expression of some lymphocyte-specific genes induced by RAG DSBs (22, 28), we hypothesized that any type of DSB can signal inhibition of RAG expression and V(D)J recombination. In this study, we demonstrate that DSBs induced in primary lymphocytes by IR or etoposide signal through ATM and Nemo to transcriptionally repress Rag1 expression and inhibit RAG

cleavage of *Igκ* loci and RSSs integrated at another genomic location. While we were preparing our manuscript, the Guikema lab reported that DSBs induced in immortalized and transformed human and mouse pre-B cell lines signal via ATM and the FOXO1 transcription factor to inhibit RAG expression and activity (29). We discuss how our study corroborates the central findings of the Guikema lab and presents novel data that provide further insights into the mechanisms and the scope by which lymphocytes direct DSB-induced feedback inhibition of V(D)J recombination. We also outline the implications of both studies to mechanisms that orchestrate the differentiation of mono-specific lymphocytes while suppressing oncogenic AgR locus translocations.

Materials and Methods

Mice

All mice used within this study were housed, bred, and used under pathogen-free conditions at the Children's Hospital of Philadelphia (CHOP). All experiments were performed using 4–6 week old mice using both male and female mice. Experimental mice were euthanized by exposure to CO_2 followed by cervical dislocation. Animal husbandry and experiments were performed in accordance with national guidelines and regulations and approved by the CHOP Institutional Animal Care and Use Committee. The *EμBCL2* (30), $Rag1^{D708A}$ (31), $Mb1Cre^{+}Atm^{flox/flox}$ (24), $VavCre^{+}p53^{flox/flox}$(32), $Mb1Cre^{+}Nemo^{flox/flox}$ (33) mice were on a mixed 129S1/SvImJ and C57BL/6 background, while $Rag1^{-/-}$ (34) and $Rag2^{-/-}$ (35) mice were on the C57BL/6 background. The wild-type control mice were of the appropriate background.

Irradiation

All mice were subject to irradiation using an XRAD320 X-ray irradiator (Precision X-Ray) and a dose rate of 0.74 Gy/min. Primary cells and cell lines were subject to irradiation using a Gammacell 1000 Cs-137 irradiator (Nordion Inc) and a dose rate of 1.8 Gy/min.

qRT-PCR quantification of Rag1, Rag2, and p21 mRNAs

Non-irradiated and irradiated cells were harvested at indicated time points and immediately lysed in Trizol (Life Technologies) and processed according to the manufacturer's instructions. Isolated RNA was treated with DNase (Promega) according to manufacturer directions, primed with random nonamers (New England Biolabs, NEB), and reverse transcribed with M-MuLV (NEB) to generate cDNA. The cDNAs were then used as template for qRT-PCR reactions were performed with SYBR green mastermix (Applied Biosystems) and run on an Applied Biosystems 7500 Fast machine. Values were normalized to housekeeping genes as indicated in the text and fold change was determined by the ΔΔCT method. The primers used for qRT-PCR reactions are listed in Supplementary Table 1. When pre-B cells were subject to irradiation, non-irradiated pre-B cells also were transported to the irradiator, but not exposed to ionizing radiation along with irradiated samples. The irradiated and non-irradiated pre-B cells were each placed back into culture until they were harvested. Since pre-B cells were transported to and from the irradiator at room temperature, the basal levels of Rag1, Rag2, and p21 mRNAs were lower at 1 hour after the irradiation time point than at 4 hours after the irradiation time point. To inactivate the ATM kinase, the KU55933

ATM kinase inhibitor was added to media at a concentration of 15 μM To block new protein synthesis, the cycloheximide ribosome inhibitor was added to media at a concentration of 10 μg/mL.

Primary pre-B cell cultures

Primary bone marrow (BM) cells were harvested by flushing BM from all leg bones of at least four mice of the appropriate genotype for each experiment. These BM cells were cultured for 3–5 days in RPMI supplemented with 10% FBS, 10 mM HEPES, 1 × non-essential amino acids, 1 mM L-glutamine, 1 mM sodium pyruvate, 100 U/mL pen-strep, 30 μM β-mercaptoethanol and 50 ng/mL IL-7. Cells were plated at a density of 5 million cells per mL of media. Each day, cells were harvested and put back into culture in fresh media at a density of 5 million cells per mL. To induce G1 arrest and activate transcription of *Rag1* and *Rag2* by IL7 withdrawal, cells were pelleted by centrifugation, re-suspended in the same media lacking IL7 at a density of 5 million cells per mL, and treated as described for each experiment.

Western blot analysis of Rag1, Rag2, and actin proteins

Pre-B cells were washed with PBS and re-suspended in ice cold lysis buffer (20 mM Tris pH 7.4, 20 mM glycerol phosphate, 10 mM sodium orthovanadatem, 10% glycerol, 0.5 mM EDTA, 0.5 mM $MgCl_2$, 200 mM NaCl, and 0.2% Triton-X) and then sonicated at intervals of 30 seconds on and 30 seconds off for 8 minutes at 4°C. The sonicated cells were incubated on ice for 10 minutes and then centrifuged to remove insoluble material. Laemmli buffer was added and then samples were boiled for 5 minutes. Lysates from equivalent numbers of pre-B cells were loaded and run on NuPage tris-glycine gels (Life Technologies). Electrophoresed proteins were transferred to Immobilon-FL PVDF membrane (EMD Millipore). Membranes were blocked with Odyssey blocking buffer (Li-Cor) according to manufacturer's instructions. Antibodies used are: anti-Rag1 or anti-Rag2 monoclonal antibody (36); anti-actin antibody (Sigma AV40173); anti-Gadd45α (Santa Cruz sc-797). Blots were washed and incubated with appropriate IRDye800 secondary antibodies (LiCor) according to manufacturer's instructions. Following washing, blots were scanned on an Odyssey infrared scanner (Li-Cor).

Click-It analysis of Rag1 and Rag2 mRNA turnover and Rag1 and Rag2 transcription

These assays were conducting using Click-It® Nascent RNA Capture kits (Life Technologies). For mRNA turnover assays, ethynyl uridine (EU) was added to medium of IL7 withdrawn pre-B cell cultures at a final concentration of 0.2 mM for the final 16 hours of culture time. Pre-B cells were washed, placed into media lacking EU, and then split into pools that were immediately irradiated or left non-irradiated. Cell pools were collected for RNA isolation immediately before EU removal or at indicated times after EU removal or EU removal and irradiation. For transcriptional assays, pre-B cells were grown in media lacking EU. Cultures were split into pools that were either irradiated or left non-irradiated. Immediately after irradiation of some pools, EU was added to the media of all pools at a final concentration of 0.5 mM. After the indicated times, cells were collected for RNA isolation. For both assays, RNA was isolated using Trizol (Life Technologies) according to the manufacturer's instructions. Click chemistry and streptavidin pull down of EU-labeled

RNA were performed according to the Click-It Nascent RNA Capture kit's instructions. Pulled-down RNA was reverse transcribed and analyzed by qRT-PCR as described above. The loading controls for mRNA turnover and transcription experiments were 18S RNA and Hprt mRNA, respectively.

Abelson pro-B cell cultures

The *EμBCL2* (A2) (37) and *Artemis*$^{-/-}$*EμBCL2* (Art2.1) (38) Abelson transformed and immortalized pro-B cell lines were previously described. We made the *EμBCL2-pINV* (39) Abelson pro-B cell line using the same procedures that we previously used to generate cell lines with recombination substrates (40). Abelsons pro-B cells were cultured in RPMI media supplemented with 10% FBS, 100 U/mL pen-strep, and 30 μM β-mercaptoethanol To induce G1 cell cycle arrest, differentiation into pre-B cells, expression of *Rag1* and *Rag2* mRNA, and V(D)J recombination, 5 μM of STI571 was added to the culture media. To induce DSBs by genotoxic drugs, etoposide was added to the media at a concentration of 10 μg/mL or bleomyin was added at a concentration of 5 μM.

Southern blot analysis

Southern blotting was performed as described (38). Briefly, 15–20 μg of genomic DNA was digested with Sac1-HF (NEB) and EcoR1-HF (NEB). Southern blot membranes were probed with a *3'Jκ* probe and then a *5'Hprt* probe as a loading control. The intensities of bands were quantified using ImageJ software (NIH). For *Artemis*$^{-/-}$*EμBLC2* cells, the percentage of *Jκ* cleavage at each time point was calculated by dividing the total intensities of *Jκ* coding end bands by the combined intensities of the germline *Jκ* band and *Jκ* coding end bands (40). For *EμBLC2* cells, the percentage of *Jκ* cleavage at each time point was calculated by dividing the intensity of the germline *Jκ* band by the intensity of the *5'Hprt* control band.

Flow cytometry

For analysis of GFP expression in *EμBCL2-pINV* cells, cells were washed in FACS buffer (PBS with 3% FCS and 0.25 mM EDTA) and then stained with PE-conjugated anti-human CD4 antibody (BD Pharmigen, clone RPA-T4) to stain cells containing the substrate. Flow cytometry was conducted using an LSR-II flow cytometer (BD Biosciences) and data was analyzed using FlowJo 10.

Statistical analyses

All statistics were performed using GraphPad Prism 5 or Prism 7 software.

Results

The suppression of Rag1 and Rag2 mRNA in response to ionizing radiation is a prevalent response of immature lymphocytes

We first sought to determine the ability of DSBs induced by ionizing radiation to suppress *Rag1* and *Rag2* expression in developing B and T lymphocytes. Since we discovered that the DDR of immature lymphocytes frequently is abnormal in immortalized cell lines and in

primary cells cultured *ex vivo* (41), we conducted initial experiments by exposing live mice to IR. To limit apoptosis of immature lymphocytes, we utilized *EμBCL2* mice with transgenic expression of the anti-apoptotic BCL2 protein in all B and T lineage cells. We exposed these mice to IR and harvested cells from their thymuses and bone marrow (BM) 1 or 4 hours later. We conducted qRT-PCR on RNA isolated from these cells or corresponding cells of non-irradiated *EμBCL2* mice. We quantified levels of Rag1 and Rag2 mRNA relative to levels of the T lineage-specific Lck mRNA for thymus or the B lineage-specific Cd19 mRNA for BM. To control for the induction of DSBs, we quantified mRNA levels of the p21 cyclin dependent inhibitor gene whose transcription is activated by ATM and Tp53 following DSBs (1). We detected lower levels of Rag1 and Rag2 mRNAs and higher levels of p21 mRNA in BM from irradiated *EμBCL2* mice as compared to BM from non-irradiated *EμBCL2* mice (Fig. 1A). The levels of Rag1 mRNA were reduced by more than 50% at 1 and 4 hours after exposure to 10 Gy of ionizing radiation, while levels of Rag2 mRNA were reduced by ~50% at both times (Fig. 1A), indicating that immature B lymphocytes rapidly inhibit *Rag1* and *Rag2* expression in response to IR. In contrast, we observed no decrease in the level of Rag1 or Rag2 mRNA in thymuses from irradiated *EμBCL2* mice relative to thymuses from non-irradiated *EμBCL2* mice, despite induction of DSBs as reflected by elevated p21 mRNA levels (Fig. 1B). Indeed, the levels of Rag1 and Rag2 mRNA each were increased by ~40% at 4 hours after exposure to 10 Gy of ionizing radiation (Fig. 1B). We corroborated that IR rapidly downregulates Rag1 and Rag2 mRNA in BM but not thymuses of wild-type mice that lack the pro-survival *EμBCL2* transgene (Fig. 1C, D). Collectively, these data suggest that DSBs induced by ionizing radiation inhibit *Rag1* and *Rag2* expression in developing B lymphocytes but not developing T lymphocytes. However, considering that BM and thymuses each contain a much greater number of pre-lymphocytes than pro-lymphocytes, this experimental approach likely is not sensitive enough to determine whether or not pro-lymphocytes downregulate *Rag1* and *Rag2* expression in response to DSBs.

We next sought to determine the effects of DSBs on *Rag1* and *Rag2* expression in primary pro-B and pro-T cells. For this purpose, we turned to $Rag1^{-/-}$ and $Rag2^{-/-}$ mice in which lymphocyte development is blocked at the pro-B and pro-T cell stages (34, 35). The $Rag1^{-/-}$ mice have a drug-resistance gene driven by a constitutive promoter in place *Rag1* coding sequences, while the $Rag2^{-/-}$ mice have a *loxP* site in place of *Rag2* coding sequences. We observed decreased levels of Rag1 mRNA in BM from irradiated $Rag2^{-/-}$ mice relative to BM from non-irradiated $Rag2^{-/-}$ mice (Fig. 1E). The levels of Rag1 mRNA in $Rag2^{-/-}$ BM were reduced ~75% at 1 hour after 10 Gy IR and ~90% at 4 hours after 10 Gy IR. Notably, we detected lower levels of Rag1 mRNA in thymuses from irradiated $Rag2^{-/-}$ mice as compared to thymuses from non-irradiated $Rag2^{-/-}$ mice (Fig. 1F). The levels of Rag1 mRNA in $Rag2^{-/-}$ thymuses were reduced ~40% at 1 and 4 hours after 10 Gy IR. Consistent with these findings, we observed that IR downregulated Rag2 mRNA in BM and thymus of $Rag1{-/-}$ mice to a similar extent as Rag1 mRNA in $Rag2{-/-}$ mice. (Supplemental Fig. 1). The results of our experiments with $Rag1^{-/-}$ and $Rag2^{-/-}$ mice suggest that DSBs downregulate *Rag1* and Rag2 expression in primary pro-B and pro-T cells.

The induction of DSBs in pre-B cells downregulates levels of Rag1 and Rag2 mRNAs

To validate that DSBs induced by ionizing radiation in primary pre-B cells downregulate *Rag1* and *Rag2* expression, we turned to the *ex vivo* culture system wherein we discovered that RAG DSBs inhibit *Rag1* and *Rag2* expression (24). The culture of primary mouse BM in media containing IL7 cytokine selectively promotes survival and proliferation of pre-B cells, such that within a few days over 95% of cells in culture are pre-B cells(42). IL7 also suppresses *Rag1* and *Rag2* expression (43). Following removal of IL7, pre-B cells arrest in G1 phase and activate *Rag1* and *Rag2* transcription (42). Expression of the *EμBCL2* transgene enables pre-B cells to survive and express *Rag1* and *Rag2* for several days after IL7 removal (42). We cultured pre-B cells from *EμBCL2* mice, removed IL7 for 48 hours to arrest cells in G1 phase and induce *Rag1* and *Rag2* transcription, exposed cells to 4 Gy IR, and then isolated RNA at 1 or 4 hours following irradiation. In parallel, we harvested RNA from non-irradiated pre-B cells. We used qRT-PCR to quantify Rag1 and Rag2 mRNA levels relative to actin mRNA levels. We also quantified p21 mRNA to confirm the induction of DSBs. We detected lower levels of Rag1 and Rag2 mRNA and higher levels of p21 mRNA in irradiated *EμBCL2* pre-B cells as compared to non-irradiated *EμBCL2* pre-B cells (Fig. 2A). The levels of Rag1 and Rag2 mRNA each were reduced ~80% at 1 and 4 hours following exposure to ionizing radiation (Fig. 2A), indicating that pre-B cells rapidly inhibit *Rag1* and *Rag2* expression in response to IR.

While our data suggest that DSBs induced by ionizing radiation inhibit *Rag1* and *Rag2* expression, they cannot rule out that other types of cellular damage caused by IR promote this response. To address this issue, instead of exposing pre-B cells to IR, we exposed cells to drugs that predominantly induce DSBs. Bleomycin is a genotoxic drug that induces DSBs throughout the cell cycle, but also damages RNA (44). We observed lower levels of Rag1 and Rag2 mRNAs and higher levels of p21 mRNA in *EμBCL2* pre-B cells treated with bleoymcin relative to *EμBCL2* pre-B cells treated with only vehicle (Fig. 2B). The levels of Rag1 and Rag2 mRNA each were reduced ~60–80% at 1 and 4 hours with treatment with bleomycin (Fig. 2B), indicating that DSBs induced in pre-B cells rapidly inhibit *Rag1* and *Rag2* expression. Etoposide is a genotoxic drug whose only demonstrated biological effect is that it inhibits re-ligation of DNA by type II topoisomerase enzymes, causing accumulation of DSBs (45). Although etoposide causes DSBs mainly in S phase cells (45), this genotoxic agent does induce DSBs in G1 arrested pre-B cells (46). We detected lower levels of Rag1 and Rag2 mRNAs and higher levels of p21 mRNA in *EμBCL2* pre-B cells treated with etoposide relative to *EμBCL2* pre-B cells treated with only vehicle (Fig. 2C). The levels of Rag1 and Rag2 mRNA each were reduced ~80% at 1 and 4 hours with treatment with etoposide (Fig. 2C), indicating that DSBs induced in pre-B cells rapidly inhibit *Rag1* and *Rag2* expression. Considering that ionizing radiation, bleomycin, etoposide, and RAG cleavage of Igκ loci (24) each suppress Rag1 and Rag2 mRNA levels, we conclude that any type of DSB activates DSB-induced feedback inhibition of *Rag1* and *Rag2* expression.

DSBs induced in pre-B cells inhibit expression of Rag1 protein but not Rag2 protein

For DSB-induced feedback inhibition of *Rag1* and *Rag2* expression to suppress V(D)J recombination, Rag1 and/or Rag2 protein levels must be diminished as a result of decreased Rag1 and Rag2 mRNA. Previous studies reported that the Rag1 and Rag2 proteins each have

a half-life of ~10–12 minutes (29, 47, 48). Considering these reports and our observed kinetics and extents of Rag1 and Rag2 mRNA loss in response to IR, one would predict appreciable decreased levels of Rag1 and Rag2 protein at 1 hour after irradiation. To confirm this prediction, we conducted western blot analysis of IL7 withdrawn primary pre-B cells at 1 and 4 hours after their exposure to 4 Gy of IR. In parallel, we assayed Rag1 and Rag2 protein in non-irradiated pre-B cells. We also conducted western blot analysis for actin protein and quantified Rag1 and Rag2 protein levels relative to actin protein. We observed reduced levels of Rag1 protein in irradiated *EμBCL2* pre-B cells as compared to non-irradiated *EμBCL2* pre-B cells (Fig. 2D). Consistent with our prediction, Rag1 protein was reduced ~50% at 1 hour after 4 Gy IR and ~75% at 4 hours after 4 Gy IR. In marked contrast, we detected no change in Rag2 protein levels after irradiation of *EμBCL2* pre-B cells (Fig. 2D), which is not consistent with our prediction. Regardless, as both Rag1 and Rag2 are required for RAG endonuclease activity (49), the downregulation of Rag1 protein levels in response to the induction of DSBs could be sufficient to inhibit V(D)J recombination.

Endogenous Rag2 protein in primary pre-B cells has an immeasurably long half-life

We found the retention of Rag2 protein following the loss of Rag2 mRNA interesting, particularly because it was not predicted from the published half-life of Rag2 protein. The possible explanations of our finding are that the basal half-life of Rag2 protein in primary pre-B cells is much longer than ~45 minutes and/or DSBs induced in primary pre-B cells increase the half-life of Rag2 protein. The Rag2 protein is expressed in G1 but not in subsequent cell cycle phases due to its phosphorylation and consequent degradation upon S phase entry (48, 50, 51), supporting the possibility that Rag2 protein might be very stable in G1 phase cells. The published half-life of Rag2 protein is only 10–12 minutes, however this value was obtained by measuring asynchronously cycling non-lymphoid cell lines with ectopic expression of Rag2 (48, 51). Therefore, we investigated the basal half-life of Rag2 protein in G1-arrested primary pre-B cells. We conducted western blot analysis of IL7 withdrawn primary pre-B cells at increasing times after addition of cycloheximide to block new protein synthesis. As a positive control for inhibition of protein synthesis, we also conducted western blot analysis of the c-Myc protein, which has a half-life of less than one hour (52). Strikingly, we detected no loss of Rag2 protein at any time point after cycloheximide addition, despite rapid loss of c-Myc protein (Fig. 2E). In this context, we could not calculate the half-life of Rag2 protein because we detected no loss of Rag2 protein levels at 24 hours after cycloheximide (Fig. 2E), following which pre-B cells begin to die from lack of new protein synthesis. Since we could not detect loss of Rag2 protein in non-irradiated cells, we were not able to ascertain the potential effect of DSBs on Rag2 protein stability.

DSBs induced in pre-B cells signal rapid transcriptional repression of Rag1 and Rag2

We next sought to elucidate mechanisms by which DSBs cause downregulation of Rag1 and Rag2 mRNA. This loss of mRNA could be due to increased turnover of Rag1 and Rag2 mRNAs and/or repression of *Rag1* and *Rag2* transcription. We utilized Click-iT mRNA capture technology to investigate these possibilities. Click-iT® mRNA capture incorporates ethylene uridine (EU) into RNAs during transcription; EU-labeled RNAs are conjugated

with biotin, isolated by streptavidin beads, and quantified by qRT-PCR. To measure turnover of Rag1 and Rag2 mRNAs in irradiated and non-irradiated primary pre-B cells, we added EU to the media of *EμBCL2* pre-B cell cultures for the last 16 hours of IL7 withdrawal to fully label existing mRNAs. We washed out EU immediately before exposure of cells to 4 Gy IR to block further EU incorporation so that we could measure the amounts of EU-labeled Rag1 and Rag2 mRNA remaining over time in irradiated and non-irradiated cells. We found that the Rag1 and Rag2 mRNAs each have a half-life of ~40 minutes (Fig. 3A), similar to published results using nuclear run-on assays on primary pre-B cells (53). At all times assayed, we detected no difference in the levels of labeled Rag1 mRNA between irradiated and non-irradiated cells (Fig. 3A), indicating that pre-B cells do not increase turnover of Rag1 mRNA in response to DSBs. In contrast, we observed lower levels of labeled Rag2 mRNA at 30 and 45 minutes following irradiation (Fig. 3A), reflecting that DSBs induced in pre-B cells decrease the half-life of Rag2 mRNA from ~40 minutes to ~30 minutes. To investigate *Rag1* and *Rag2* transcription, we added EU to IL7-withdrawn *EμBCL2* pre-B cells immediately after exposure to 4 Gy IR. We also added EU to non-irradiated IL7-withdrawn *EμBCL2* pre-B cells. Over time, we measured the amounts of newly synthesized, EU-labeled Rag1 and Rag2 mRNA, and the loading control Hprt mRNAs. In this experiment, the balance of transcription and mRNA turnover determines the amount of a labeled mRNA. By 45 minutes after irradiation, we observed near complete loss of labeled Rag1 and Rag2 mRNAs in irradiated cells relative to non-irradiated cells (Fig. 3B). Considering the ~30–40 minute turnover of Rag1 and Rag2 mRNAs in irradiated pre-B cells (Fig. 3A), the kinetics and extents by which EU-labeled Rag1 and Rag2 mRNAs are lost in irradiated cells suggests that DSBs cause an immediate halt of *Rag1* and *Rag2* transcription.

To investigate whether DDR activation in immature lymphocytes leads to repression of genes non-essential to the genotoxic stress response, we also measured the amount of newly synthesized, EU-labeled *Wasp* mRNA since Wasp has no documented role in the DDR and irradiation of primary pre-B cells has no effect on steady-state mRNA levels (data not shown). Our analysis reveals that irradiation of primary pre-B cells has minimal effect on the synthesis of Wasp mRNA (Fig. 3B). Thus, we conclude that *Rag1* and *Rag2* transcription is specifically targeted by the DDR, and not simply part of a generalized inhibition of transcription in the presence of widespread DNA damage.

Consistent with the rapid timeframe of *Rag1*and *Rag2* transcriptional suppression, inhibition of new protein synthesis by cycloheximide treatment does not prevent the loss of Rag1 and Rag2 mRNA levels following irradiation of *EμBCL2* pre-B cells (Fig. 3C). This finding suggests that DSBs suppress *Rag1* and *Rag2* transcription through factors constitutively expressed in primary pre-B cells. Collectively, these data are consistent with repression of *Rag1* and *Rag2* transcription being the predominant mechanism by which pre-B cells signal DSB-induced loss of *Rag1* and *Rag2* expression.

DSB-induced downregulation of Rag1 and Rag2 expression requires the ATM kinase

We next launched a line of research to elucidate the factors by which DSBs induced in primary pre-B cells suppress *Rag1* and *Rag2* transcription. We previously reported that RAG

DSBs induced in pre-B cells signal via ATM to downregulate *Rag1* and *Rag2* expression (24). Therefore, we investigated the role of ATM through chemical inhibition of the ATM kinase or genetic inactivation of the ATM protein. First, we added the ATM kinase inhibitor KU55933 or vehicle only at the same time that we removed IL7 from *EμBCL2* pre-B cell cultures; 48 hours later we exposed cells to 4 Gy IR or left them untreated, and then harvested cells for qRT-PCR quantification of Rag1 and Rag2 mRNA. We also quantified p21 mRNA as a control for both induction of DSBs and inactivation of the ATM kinase, since genetic deletion of ATM impairs but does not block the ability of DSBs to induce p21 mRNA levels (54). We detected ~2–3-fold higher levels of Rag1 and Rag2 mRNAs in non-irradiated cells treated with KU55933 versus vehicle only (Fig. 4A), likely reflecting ATM-dependent suppression of *Rag1* and *Rag2* transcription from DSBs induced by RAG during *Igκ* recombination and by other transcription and cellular metabolites. Notably, the addition of KU55933 also blocked downregulation of *Rag1* and *Rag2* mRNA following irradiation (Fig. 4A). Next, we analyzed primary pre-B cells cultured from $Mb1Cre^{+}Atm^{flox/flox}$ mice with B lineage-specific conditional deletion of *Atm* initiating at the pro-B cell stage (24). Unirradiated $Mb1Cre^{+}Atm^{flox/flox}$ IL-7 withdrawn pre-B cells expressed ~2-fold higher levels of Rag1 and Rag2 mRNAs compared to *EμBCL2* pre-B cells (data not shown), possibly reflecting ATM-dependent inhibition of *Rag1* and *Rag2* expression from DSBs. Moreover, irradiation of $Mb1Cre^{+}Atm^{flox/flox}$ pre-B cells caused no change in Rag1 and Rag mRNA levels relative to non-irradiated $Mb1Cre^{+}Atm^{flox/flox}$ pre-B cells (Fig. 4B). The retention of Rag1 and Rag2 mRNA from 1–4 hours after irradiation of pre-B cells that lack ATM indicates that IR-induced DSBs signal through ATM to downregulate *Rag1* and *Rag2* expression.

DSB-induced Rag1 and Rag2 suppression does not depend on suppression of Gadd45α expression

The intracellular signaling pathways through which ATM represses gene transcription remain incompletely characterized. We previously reported that RAG DSBs induced in primary pre-B cells signal via ATM to decrease levels of Gadd45α mRNA and protein (24). Since Gadd45α had been shown to signal Foxo1-dependent transcription of Rag1 and Rag2 in an immortalized mouse pre-B cell line (25), our findings supported a model wherein DSBs suppress *Rag1* and *Rag2* transcription through ATM-mediated downregulation of Gadd45α mRNA. To investigate this model, we studied the effects of DSBs induced by IR in primary pre-B cells on Gadd45α mRNA levels. Although we found that Gadd45α mRNA levels are decreased following irradiation of *EμBCL2* pre-B cells (Supplemental Fig. 2A, B), the slow kinetics and limited extent of this response suggest that downregulation of Gadd45α mRNA is not a driving force in suppressing *Rag1* and *Rag2* expression (compare Fig. 3B and Supplemental Fig. 2B). Consistent with this notion, we observed that ectopic retroviral expression of Gadd45α in a mouse pre-B cell line does not prevent DSB-induced inhibition of *Rag1* and *Rag2* expression (Supplemental Fig. 2C). However, it is important to note that while our data argue against a role for downregulation of Gadd45α expression in DSB-induced inhibition of *Rag1* and *Rag2* transcription in response to DSBs, our experiments do not address the possibility for inactivation of Gadd45α protein activity by post-translational modifications or other mechanisms.

DSB-induced downregulation of Rag1 and Rag2 expression requires the NF-κB essential modulator protein

In pre-B cells, ATM activates transcription of target genes through Tp53-mediated or Nemo-mediated intracellular signaling pathways (1, 22). Thus, we next investigated the roles of Tp53 and Nemo in suppressing *Rag1* and *Rag2* expression following the induction of DSBs in primary pre-B cells. We observed normal downregulation of Rag1 and Rag2 mRNAs following irradiation of primary pre-B cells cultured from $VavCre^{+}Tp53^{flox/flox}$ mice with hematopoietic lineage-specific deletion of *Tp53* (Supplemental Fig. 2E)(32). In contrast, we detected impairment of this DSB response in pre-B cells from $Mb1Cre^{+}Nemo^{flox/flox}E\mu BCL2$ mice with B lineage-specific *Nemo* deletion and ectopic BCL2 expression to enhance survival of *Nemo*-deficient pre-B cells (Fig. 5A)(33). Although the Rag1 and Rag2 mRNA levels at 4 hours following IR were equivalent to unirradiated cells, the levels at 1 hour after IR were decreased as compared to unirradiated cells (Fig. 5A). However, this downregulation of Rag1 and Rag2 mRNA in $Mb1Cre^{+}Nemo^{flox/flox}E\mu BCL2$ pre-B cells at 1 hour following IR is to a lesser extent than in *EμBCL2* pre-B cells (Fig. 5B). Our data indicate that Nemo is required for normal DSB-induced feedback inhibition of *Rag1* and *Rag2* expression in pre-B cells, with the absence of Nemo resulting in slower kinetics by which pre-B cells downregulate *Rag1* and *Rag2* expression upon irradiation. This finding suggests a two-phase regulation of *Rag1* and *Rag2* transcription in response to DSBs: an early initiation phase that is partially dependent on Nemo and a later maintenance phase that requires Nemo expression.

DSBs induced in pre-B cells by genotoxic drugs inhibit V(D)J recombination of Igκ loci and an integrated substrate

After demonstrating that DSBs induced by IR or genotoxic drugs inhibit *Rag1* and *Rag2* expression, we sought to test our hypothesis that these types of DSBs inhibit V(D)J recombination. For this purpose, we etoposide and bleomycin since these drugs are active for days in cell culture, which is the time frame over which can activate and monitor V(D)J recombination in primary pre-B cells or pre-B cell lines. We first attempted to study the effect of etoposide-induced DSBs on *Igκ* recombination in primary *EμBCL2* pre-B cells; unfortunately, all of the etoposide doses that we tested caused substantial apoptosis. To circumvent this obstacle, we turned to the Abelson transformed (abl) pro-B cell lines that we had previously used to identify RAG DSB-induced feedback inhibition of *Igκ* recombination and to study additional cellular responses to RAG DSBs (38, 40). In normal media, Abl pro-B cells proliferate and only sporadically express *Rag1* and *Rag2* and recombine *Igκ* loci (55). Addition of the STI571 Abelson kinase inhibitor causes G1 cell cycle arrest and differentiation of pre-B cells that express *Rag1* and *Rag2* and recombine *Igκ* loci (55). Expression of the *EμBCL2* transgene enables Abl cells to survive RAG DSBs and transcribe *Rag1* and *Rag2* for several days (37). Moreover, the addition of etoposide to STI571-treated, G1-arrested Abl cells induces DSBs (46). We found that addition of etoposide at 24 hours after STI571 addition had minimal effects on G1 arrest and survival of Abl cells over the next 48 hours. Consistent with our data from primary *EμBCL2* pre-B cells (Fig. 2B), the addition of etoposide to *EμBCL2* Abl cells caused downregulation of Rag1 and Rag2 mRNA and upregulation of p21 mRNA (Fig. 6A). The small size of the *Jκ* cluster enables the use of Southern blot analysis to monitor *Igκ* recombination. In *EμBCL2* Abl cells, we measure *Igκ*

recombination by quantifying decreased intensity of the germline *Jκ* band relative to the intensity of control band from a non-rearranging locus. Our Southern blot analysis revealed that the addition of etoposide 24 hours after activating *Igκ* recombination in *EμBCL2* Abl cells inhibited further *Igκ* recombination over the next 48 hours (Fig. 6B). We conducted the same experiment with *EμBCL2* pre-B cell lines lacking the Artemis NHEJ factor, which is required for coding join formation (56). The addition of etoposide to Artemis$^{-/-}$*EμBCL2* Abl cells caused downregulation of Rag1 and Rag2 mRNA and upregulation of p21 mRNA (Fig. 6C). In Artemis$^{-/-}$*EμBCL2* Abl cells, we measure RAG cleavage of *Igκ* loci by quantifying the relative intensity of germline *Jκ* bands and *Jκ* coding end bands (57). We found that addition of etoposide 24 hours after activating RAG cleavage of *Igκ* loci in *Artemis*$^{-/-}$*EμBCL2* Abl cells blocked further RAG cleavage of *Igκ* loci over the next 48 hours (Fig. 6D). We repeated this same experiment by substituting bleomycin for etoposide. We observed that the addition of bleomycin 24 hours after activating RAG cleavage of endogenous *Igκ* loci in *Artemis*$^{-/-}$*EμBCL2* Abl cells also blocked further RAG cleavage of *Igκ* loci over the next 48 hours (Supplemental Figure 3). These data demonstrate that DSB induced by etoposide or bleomycin in pre-B cells activates DSB-induced feedback inhibition of RAG cleavage to initiate *Igκ* recombination.

The Sleckman laboratory recently reported a locus-specific *trans*-factor for RAG DSB-induced feedback inhibition of *Igκ* recombination that functions by downregulating transcription-linked accessibility of *Jκ* gene segments to the RAG endonuclease (27). In this context, the ability of etoposide to inhibit *Igκ* recombination could be due to downregulation of *Rag1* and *Rag2* expression and/or *Jκ* recombinational accessibility. Therefore, we thought it was important to determine whether DSB-induced feedback inhibition in pre-B cells also suppresses recombination of RSSs inserted at another genomic location. For this purpose, we turned to *EμBCL2* Abl cells containing one chromosomally integrated copy of the pINV recombination substrate. The pINV substrate contains a constitutive promoter, and a downstream GFP cDNA oriented in the anti-sense reading frame that is flanked by compatible RSSs (37, 58). The orientation of these RSSs is such that V(D)J recombination inverts the GFP cDNA, leading to GFP expression (37, 58). Due to sporadic Rag1 and Rag2 expression during culture, a small fraction (~10%) of *EμBCL2-pINV* cells expresses GFP before the addition of STI571. The addition of etoposide but not vehicle only 24 hours after STI571 addition to *EμBCL2-pINV* Abl cells resulted in lower levels of Rag1 and Rag2 mRNA and higher levels of p21 mRNA after an additional 48 hours of culture (Fig. 6E). Reflecting this suppression of *Rag1* and *Rag2* expression, flow cytometry analysis revealed that etoposide suppressed generation of GFP^{+} cells (Fig. 6F). These data indicate that DSB-induced feedback inhibition of V(D)J recombination in pre-B cells occurs independent of *Igκ*-specific *trans*-factors.

Discussion

Our study demonstrates that immature lymphocytes downregulate *Rag1* and *Rag2* expression and inhibit V(D)J recombination in response to DNA damage. The suppression of Rag1 and Rag2 mRNA levels following ionizing radiation is a response shared by pro-T, pro-B, and pre-B cells. Where assayed, this response is dependent on the ATM kinase and also triggered by etoposide or bleomycin, providing strong evidence that immature

lymphocytes experiencing DSBs inhibit *Rag1* and *Rag2* expression. Our use of a primary mouse pre-B cell culture system enabled us to elucidate that transcriptional repression, rather than induction of mRNA turn over, is the mechanism by which DSBs downregulate *Rag1* and *Rag2* expression. This inhibition is immediate, not requiring protein synthesis, and causes rapid loss in protein levels of Rag1 but not Rag2. Since both Rag1 and Rag2 protein are required for RAG endonuclease activity (12, 49), DSBs induced in pre-B cell lines by etoposide inhibit recombination of endogenous *Igκ* loci and a chromosomally integrated artificial substrate. These data build on our prior work demonstrating that RAG DSBs induced during *Igκ* recombination in a primary pre-B cell signal through ATM to downregulate levels of Rag1 and Rag2 mRNAs and Rag1 protein and to feedback inhibit additional RAG cleavage of *Igκ* gene segments (24). Based on our current and prior findings, we conclude that any type of DSB induced anywhere in the genome of a pre-B cell has the potential to signal immediate cessation of *Rag1* and *Rag2* transcription, leading to rapid downregulation of Rag1 protein expression and thereby V(D)J recombination throughout the nucleus. Considering that immature T cells express an order of magnitude fewer number of Rag1 monomers than Rag2 monomers (59), DSB-induced downregulation of Rag1 protein in immature lymphocytes would be predicted to be a more effective way to reduce RAG activity than downregulation of Rag2 protein. In this context, the retention of Rag2 protein in thymocytes harboring RAG DSBs at TCR loci (60) may result from a long half-life of endogenous Rag2 protein enabling Rag2 to persists following DSB-induced repression of *Rag1/Rag2* transcription and resultant loss of Rag1 protein. While RAG induces two DSBs at an *Igκ* allele, the IR dose and etoposide concentration that we used in our pre-B cell experiments each induce hundreds of DSBs at random genomic locations (61, 62). Considering that two DSBs induced by RAG during *Igκ* recombination and a larger number of DSBs induced by IR or etoposide cause similar reduction in *Rag1* and *Rag2* mRNA levels, it will be important to assess whether intrinsic features of the RAG proteins or the location, proximity, of structures of the two DSBs induced by RAG during *Igκ* recombination amplify DDR signaling.

Our data that both ATM and Nemo are required for ionizing radiation to rapidly suppress *Rag1* and *Rag2* mRNA levels in primary pre-B cells implicates a role for canonical NF-κB transcription factors. In pre-B cells, DSBs induced by RAG or etoposide signal ATM-dependent and Nemo-dependent nuclear translocation and DNA binding of canonical NF-κB proteins to upregulate or downregulate expression of numerous genes (22). The post-translational modification of Nemo upon DSBs or other stimuli is essential for rapid cytoplasmic-to-nuclear migration of canonical NF-κB proteins, promoting NF-κB-mediated transcriptional activation or repression of target genes (3, 63–65). The canonical NF-κB proteins consist of p50, p65, and c-Rel, which each can function as homodimers or as heterodimers with each other or with additional transcription factors (63–65). Unlike p65 and c-Rel, p50 lacks a transactivation domain and forms homodimers that repress transcription (63, 66, 67). The mechanisms by which DSBs and other stimuli direct the formation of specific NF-κB complexes and target these to particular gene promoters remain enigmatic (63–65). Several studies have investigated the role of NF-κB proteins in regulating *Rag1/Rag2* expression in immature B cells, reaching apparently contradictory conclusions. In immortalized and transformed cell lines, the expression of a dominant

negative IκBα protein that sequesters canonical NF-κB proteins in the cytoplasm either has no effect or increases sporadic *Rag1/Rag2* expression depending on the lines analyzed (68, 69). The inhibition of canonical NF-κB activity in primary pre-B cells by expression of the same dominant negative IκBα protein or by *Mb1Cre*-mediated deletion of *Nemo* has no effect on *Rag1* and *Rag2* mRNA levels, even after IL7 withdrawal (33). However, the expression of a different dominant negative IκBα protein in primary pre-B cells inhibits antibody-stimulated BCR signaling from inducing *Rag1/Rag2* transcription (53). ChIP analyses revealed that p50, p65, and c-Rel each bind at several sites along the *Rag1/Rag2* locus, including the ERag B cell specific enhancer and the D3 lymphoid specific enhancer, with BCR activation increasing p65 and c-Rel binding and decreasing p50 binding (53). Moreover, pre-B cells from mice with inactivation of the *Nfkb1* gene that encodes p50 exhibit higher basal and BCR-stimulated expression of *Rag1* and *Rag2* (53). Collectively, our data and these prior findings support a model wherein a balance of positive-acting (p65/c-Rel) and negative-acting (p50) canonical NF-κB proteins helps regulate *Rag1* and *Rag2* transcription in pre-B cells, with increased binding of p50 in response to DSBs repressing *Rag1/Rag2* transcription. However, considering that Nemo can function independent of NF-κB proteins (70, 71), DSBs induced in pre-B cells might repress *Rag1* and *Rag2* expression through other Nemo-mediated signaling pathways. Another alternative possibility is that Nemo-dependent NF-κB activity is necessary for constitutive expression of ATM-dependent signaling factors and/or transcriptional repressor that target the *Rag1/Rag2* locus.

While we were preparing this manuscript, the Guikema lab reported that the DDR response regulates *Rag1/Rag2* expression in pre-B cells through ATM-FOXO1 signaling (29). They showed that the genotoxic drug NCS caused rapid downmodulation of Rag1 and Rag2 mRNA and Rag1 protein (they did not report on Rag2 protein) in STI571-treated human BCR-ABL$^+$ pre-B cell lines (BV173 and SUP-B15) and mouse v-Abl transformed pro-B cell lines. Consistent with data from primary mouse pre-B cells (47) the half-life of RAG1 in BV173 cells is relative short (<60 minutes). NCS causes a modest decrease of RAG1 half-life in BV173 cells, but does not affect levels of Rag1 protein expressed in a human embryonic kidney cell line, consistent with transcriptional repression being the mechanism by which DNA damage downmodulates RAG1 protein. Inhibition of ATM kinase activity antagonized the ability of NCS to downregulate Rag1 mRNA levels in pre-B cell lines and primary pre-B cells. NCS promotes both the ATM kinase-dependent loss of FOXO1 binding to ERag and the binding of phospho-ATM to ERag. Since FOXO1 and un-activated ATM are frequently in close proximity, the Guikema lab proposes a model wherein DSBs activate ATM to release FOXO1 binding from ERag and thereby repress *Rag1/Rag2* transcription. Finally, they showed that inhibition of ATM kinase activity elevated Rag1 mRNA levels in immature B cell lines and increased sporadic recombination of a retroviral substrate in a pre-B cell line, implying that RAG DSB-induced loss of Rag1 protein expression inhibits V(D)J recombination.

Our work corroborates central findings of the Guikema lab and presents additional data that provide substantial insights into potential mechanisms by which immature lymphocytes direct DSB-induced feedback inhibition of V(D)J recombination. Both studies show that DSBs induced by a genotoxic drug in pre-B cells signal via ATM to rapidly downregulate

Rag1 and *Rag2* expression, but we also show that this DSB response occurs independent of new protein synthesis and involves transcriptional repression of the *Rag1/Rag2* locus. In addition, we demonstrate that expression of the Nemo protein is required for normal DSB-induced feedback inhibition of *Rag1* and *Rag2* expression in pre-B cells, with the absence of Nemo possibly resulting in slower kinetics by which pre-B cells suppress *Rag1* and *Rag2* expression in response to DSBs. When considered with work of the Guikema lab, our data is consistent with a model wherein ATM-FOXO1 and ATM-Nemo signaling cooperate to rapidly initiate *Rag1/Rag2* transcriptional repression, while ATM-Nemo signaling maintains this response. In this context, the release of FOXO1 might facilitate NF-κB binding and/or *vice versa*; while NF-κB binding may more stably inhibit *Rag1/Rag2* expression, such as by persisting longer after cessation of ATM kinase activity following DSB repair. As highlighted by our prior (24) and current Gadd45α data, a potential mechanistic link between release of FOXO1 and inhibition of *Rag1/Rag2* transcription should be assessed to distinguish a cause-effect relationship versus another unlinked ATM-dependent correlation. Considering the complexities of ATM-FOXO1 signaling found by the Guikema lab (29), and the unresolved questions over the roles of Nemo and NF-κB proteins in *Rag1/Rag2* transcription, major obstacles exist for testing these models. Further characterization of the molecular requirements and associated events of DSB-induced inhibition of *Rag1/Rag2* expression should open paths forward.

Our findings that irradiation causes downregulation of Rag1 and Rag2 mRNA levels in pro-B cells, pre-B cells, and pro-T cells, but not in total thymocytes, have important implications for mechanisms by which immature lymphocytes regulate V(D)J recombination. One explanation for this difference between pro-T cells and total thymocytes is that pre-T cells ($CD4^+CD8^+$ thymocytes) assembling *TCRα* genes are not able to downregulate *Rag1* and *Rag2* expression in response to DSBs. In this scenario, our data may reflect the existence of developmental stage-specific mechanisms by which immature T cells regulate *Rag1/Rag2* transcription in response to DSBs. Such putative mechanisms could involve differential expression or activity of DDR factors that suppress *Rag1/Rag2* transcription or dominant roles of *cis*-regulatory elements that drive transcription of *Rag1* and *Rag2* in pre-T cells (72). An inability of pre-T cells to inhibit *Rag1* and *Rag2* expression in response to DSBs would be unique among the types of immature B and T cells that assemble AgR genes. Mirroring this, *TCRα* gene assembly in pre-T cells is not regulated to enforce allelic exclusion, whereas recombination of the only or predominant AgR genes assembled in pro-B cells (*IgH*), pre-B cells (*Igκ*), and pre-T cells (*TCRβ*) is controlled to occur on one allele at a time (73). However, an important caveat to note is that our data cannot rule out that pre-T cells experiencing DSBs from 10 Gy of radiation do not suppress *Rag1* and *Rag2* transcription because they are directly induced to die. We previously reported that mice lacking ATM develop greater frequencies of mature lymphocytes expressing *Igκ, IgH*, or *TCRβ* genes from both alleles (24, 26). These findings provided evidence for RAG DSB-induced feedback inhibition of *IgH, Igκ*, and *TCRβ* recombination (24, 26, 57). Yet, as we noted, the slower kinetics of coding join formation in cells lacking ATM could cause this increased allelic inclusion, rather than feedback inhibition of V(D)J recombination through transcriptional repression of *Rag1/Rag2* (26). Our current data show that DSBs induced in pro-B, pre-B, and pro-T cells indeed suppress *Rag1* and *Rag2* expression, providing

additional support for our model wherein the responses of these immature lymphocytes to RAG DSBs is one essential mechanism for enforcing AgR allelic exclusion (26). The additional essential mechanisms likely include inefficient Vβ and V_H RSSs (58), Ccnd3-mediated cell cycle progression (26), unequal accessibility of Ig/TCR alleles (74–76), and segregation of Ig/TCR alleles from Rag2 protein (60).

Although our data suggest that ATM-mediated downregulation of Rag1 protein expression is a mechanism by which DSBs inhibit V(D)J recombination, we have not investigated potential direct effects of ATM on suppressing AgR gene assembly. For example, ATM phosphorylation of Rag1 and/or Rag2 protein might inactivate RAG endonuclease activity prior to the reduction of Rag1 protein levels. Both Rag1 and Rag2 contain SQ/TQ motifs that could be phosphorylated by ATM and/or the related DNA-PK protein kinase. In fact, DNA-PK can phosphorylate Rag2 on Ser265 *in vitro* (77). While mutation of all of these motifs to the non-phosphorylatable AQ motif does not impair RAG endonuclease activity or V(D)J recombination in another way (39, 78), the role for phosphorylation of these SQ/TQ motifs in inhibiting RAG cleavage activity has not been reported. Considering that the AMP-activated protein kinase directly phosphorylates Rag1 to enhance the endonuclease activity of RAG1/RAG2 complexes (79), it is conceivable that ATM phosphorylation of Rag1 and/or Rag2 directly suppresses the ability of RAG to bind and/or cleave DNA. Moreover, the ability of ATM to signal nuclear export of a fraction of nuclear Rag2 protein in response to DSBs (46) opens the possibility that ATM might regulate the subcellular location of Rag1 protein. Finally, the finding of the Guikema lab (29) that the genotoxic drug neocarzinostatin increases the degradation of Rag1 protein suggests that ATM also might regulate the stability of Rag1. Clearly, studies are needed to investigate the potential role of ATM-dependent post-translational modifications of the Rag1 and Rag2 proteins in DSB-induced inhibition of V(D)J recombination.

The conservation of DSB-induced feedback inhibition of *Rag1* and *Rag2* expression among different types of immature lymphocytes and between humans and mice implies that this process is important. As we have outlined previously, it is possible that transiently suppressing RAG-mediated DNA cleavage in response to RAG DSBs induced during V(D)J recombination is critical to suppress autoimmunity from allelic inclusion and leukemia/lymphoma from oncogenic AgR locus translocations (24, 26, 73). The ability of non-RAG DSBs to inhibit RAG-mediated cleavage of an AgR locus could be a byproduct of evolutionary selection for mechanisms that enable RAG DSBs to direct mono-allelic recombination of *Igκ, IgH*, and *TCRβ* loci. In pre-T cells, RAG (and non-RAG) DSBs might signal post-translational inhibition of RAG activity and/or repression of TCRα recombination potential. Alternatively, unique requirements for TCRα recombination may have selected for mechanisms that prevent DSB-induced inhibition of V(D)J recombination. Cells that assemble AgR genes via RAG DSB intermediates also experience DSBs from other endogenous factors such as transcription and cellular metabolism. While one DSB can cause a translocation, a second simultaneous DSB increases translocation frequencies by several orders of magnitude (80). Therefore, regardless of whether the ability of immature lymphocytes to downregulate RAG activity in response to non-RAG DSBs is fortuitous, this cellular response likely helps suppress oncogenic AgR locus translocations.

Supplementary Material

Refer to Web version on PubMed Central for supplementary material.

Acknowledgments

This research was supported by the T32 AR007442 Training Program in Rheumatic Diseases of the University of Pennsylvania and NRSA grant F31 CA183551 (M.R.F), the GM007229 T32 Training Program in Cell and Molecular Biology of the University of Pennsylvania (A.R.-R.), NIH grant R37 AI32524 (D.G.S.), and the Department of Pathology and Laboratory Medicine of the Children's Hospital of Philadelphia and NIH R01 grant AI112621 (C.H.B).

References

1. Shiloh Y, Ziv Y. The ATM protein kinase: regulating the cellular response to genotoxic stress, and more. Nat. Rev. Mol. Cell Biol. 2013; 14:197–210.
2. Helmink BA, Sleckman BP. The Response to and Repair of RAG-Mediated DNA Double-Strand Breaks. Annu. Rev. Immunol. 2012; 30:175–202. [PubMed: 22224778]
3. McCool KW, Miyamoto S. DNA damage-dependent NF-κB activation: NEMO turns nuclear signaling inside out: DNA damage-dependent NF-κB activation. Immunol. Rev. 2012; 246:311–326. [PubMed: 22435563]
4. Barlow C, Hirotsune S, Paylor R, Liyanage M, Eckhaus M, Collins F, Shiloh Y, Crawley JN, Ried T, Tagle D, Wynshaw-Boris Anthony. Atm-deficient mice: a paradigm of ataxia telangiectasia. Cell. 1996; 86:159–171. [PubMed: 8689683]
5. Taylor AM, Metcalfe JA, Thick J, Mak YF. Leukemia and lymphoma in ataxia telangiectasia. Blood. 1996; 87:423–438. [PubMed: 8555463]
6. Elson A, Wang Y, Daugherty CJ, Morton CC, Zhou F, Campos-Torres J, Leder P. Pleiotropic defects in ataxia-telangiectasia protein-deficient mice. Proc. Natl. Acad. Sci. U. S. A. 1996; 93:13084–13089. [PubMed: 8917548]
7. Xu Y, Ashley T, Brainerd EE, Bronson RT, Meyn MS, Baltimore D. Targeted disruption of ATM leads to growth retardation, chromosomal fragmentation during meiosis, immune defects, and thymic lymphoma. Genes Dev. 1996; 10:2411–2422. [PubMed: 8843194]
8. Borghesani PR, Alt FW, Bottaro A, Davidson L, Aksoy S, Rathbun GA, Roberts TM, Swat W, Segal RA, Gu Y. Abnormal development of Purkinje cells and lymphocytes in Atm mutant mice. Proc. Natl. Acad. Sci. U. S. A. 2000; 97:3336–3341. [PubMed: 10716718]
9. Keeney S, Lange J, Mohibullah N. Self-organization of meiotic recombination initiation: general principles and molecular pathways. Annu. Rev. Genet. 2014; 48:187–214. [PubMed: 25421598]
10. Alt FW, Zhang F-L, Meng Y, Guo C, Schwer B. Mechanisms of Programmed DNA Lesions and Genomic Instability in the Immune System. Cell. 2013; 152:417–429. [PubMed: 23374339]
11. Tonegawa S. Somatic generation of antibody diversity. Nature. 1983; 302:575–581. [PubMed: 6300689]
12. Schatz DG, Swanson PC. V(D)J Recombination: Mechanisms of Initiation. Annu. Rev. Genet. 2011; 45:167–202. [PubMed: 21854230]
13. Notarangelo LD, Kim M-S, Walter JE, Lee YN. Human RAG mutations: biochemistry and clinical implications. Nat. Rev. Immunol. 2016; 16:234–246. [PubMed: 26996199]
14. Woodbine L, Gennery AR, Jeggo PA. The clinical impact of deficiency in DNA non-homologous end-joining. DNA Repair. 2014; 16:84–96. [PubMed: 24629483]
15. Feeney AJ, Atkinson MJ, Cowan MJ, Escuro G, Lugo G. A defective Vkappa A2 allele in Navajos which may play a role in increased susceptibility to haemophilus influenzae type b disease. J. Clin. Invest. 1996; 97:2277–2282. [PubMed: 8636407]
16. Bassing CH, Swat W, Alt FW. The mechanism and regulation of chromosomal V (D) J recombination. Cell. 2002; 109:S45–S55. [PubMed: 11983152]
17. Nemazee D. Receptor editing in lymphocyte development and central tolerance. Nat. Rev. Immunol. 2006; 6:728–740. [PubMed: 16998507]

18. Xiong N, Raulet DH. Development and selection of gammadelta T cells. Immunol. Rev. 2007; 215:15–31. [PubMed: 17291276]
19. Perkins EJ. Sensing of intermediates in V(D)J recombination by ATM. Genes Dev. 2002; 16:159–164. [PubMed: 11799059]
20. Dujka ME, Puebla-Osorio N, Tavana O, Sang M, Zhu C. ATM and p53 are essential in the cell-cycle containment of DNA breaks during V(D)J recombination in vivo. Oncogene. 2010; 29:957–965. [PubMed: 19915617]
21. Callén E, Jankovic M, Difilippantonio S, Daniel H-T, Chen JA, Celeste A, Pellegrini M, McBride K, Wangsa D, Bredemeyer AL, Sleckman BP, Ried T, Nussenzweig M, Nussenzweig A. ATM Prevents the Persistence and Propagation of Chromosome Breaks in Lymphocytes. Cell. 2007; 130:63–75. [PubMed: 17599403]
22. Bredemeyer AL, Helmink BA, Innes CL, Calderon B, McGinnis LM, Mahowald GK, Gapud EJ, Walker LM, Collins JB, Weaver BK, Mandik-Nayak L, Schreiber RD, Allen PM, May MJ, Paules RS, Bassing CH, Sleckman BP. DNA double-strand breaks activate a multi-functional genetic program in developing lymphocytes. Nature. 2008; 456:819–823. [PubMed: 18849970]
23. Bednarski JJ, Nickless A, Bhattacharya D, Amin RH, Schlissel MS, Sleckman BP. RAG-induced DNA double-strand breaks signal through Pim2 to promote pre–B cell survival and limit proliferation. J. Exp. Med. 2012; 209:11–17. [PubMed: 22201128]
24. Steinel NC, Lee B-S, Tubbs AT, Bednarski JJ, Schulte E, Yang-Iott KS, Schatz DG, Sleckman BP, Bassing CH. The Ataxia Telangiectasia mutated kinase controls Igκ allelic exclusion by inhibiting secondary *V*κ-to-*J*κ rearrangements. J. Exp. Med. 2013; 210:233–239. [PubMed: 23382544]
25. Amin RH, Schlissel MS. Foxo1 directly regulates the transcription of recombination-activating genes during B cell development. Nat. Immunol. 2008; 9:613–622. [PubMed: 18469817]
26. Steinel NC, Fisher MR, Yang-Iott KS, Bassing CH. The Ataxia Telangiectasia Mutated and Cyclin D3 Proteins Cooperate To Help Enforce TCR and IgH Allelic Exclusion. J. Immunol. 2014; 193:2881–2890. [PubMed: 25127855]
27. Bednarski JJ, Pandey R, Schulte E, White B-R, Chen LS, Sandoval GJ, Kohyama M, Haldar M, Nickless A, Trott A, Cheng G, Murphy KM, Bassing CH, Payton JE, Sleckman BP. RAG-mediated DNA double-strand breaks activate a cell type-specific checkpoint to inhibit pre–B cell receptor signals. J. Exp. Med. 2016; 213:209–223. [PubMed: 26834154]
28. Innes CL, Hesse JE, Palii SS, Helmink BA, Holub AJ, Sleckman BP, Paules RS. DNA damage activates a complex transcriptional response in murine lymphocytes that includes both physiological and cancer-predisposition programs. BMC Genomics. 2013; 14:163. [PubMed: 23496831]
29. Ochodnicka-Mackovicova K, Bahjat M, Maas C, van der Veen A, Bloedjes TA, de Bruin AM, van Andel H, Schrader CE, Hendriks RW, Verhoeyen E, Bende RJ, van Noesel CJM, Guikema JEJ. The DNA Damage Response Regulates RAG1/2 Expression in Pre-B Cells through ATM-FOXO1 Signaling. J. Immunol. 2016
30. Strasser A, Whittingham S, Vaux DL, Bath ML, Adams JM, Cory S, Harris AW. Enforced BCL2 expression in B-lymphoid cells prolongs antibody responses and elicits autoimmune disease. Proc. Natl. Acad. Sci. U. S. A. 1991; 88:8661–8665. [PubMed: 1924327]
31. Ji Y, Resch W, Corbett E, Yamane A, Casellas R, Schatz DG. The In Vivo Pattern of Binding of RAG1 RAG2 to Antigen Receptor Loci. Cell. 2010; 141:419–431. [PubMed: 20398922]
32. DeMicco A, Yang-Iott K, Bassing CH. Somatic inactivation of Tp53 in hematopoietic stem cells or thymocytes predisposes mice to thymic lymphomas with clonal translocations. Cell Cycle. 2013; 12:3307–3316. [PubMed: 24036547]
33. Derudder E, Cadera EJ, Vahl JC, Wang J, Fox CJ, Zha S, van Loo G, Pasparakis M, Schlissel MS, Schmidt-Supprian M, Rajewsky K. Development of immunoglobulin λ-chain–positive B cells, but not editing of immunoglobulin κ-chain, depends on NF-κB signals. Nat. Immunol. 2009; 10:647–654. [PubMed: 19412180]
34. Mombaerts P, Iacomini J, Johnson RS, Herrup K, Tonegawa S, Papaioannou VE. RAG-1-deficient mice have no mature B and T lymphocytes. Cell. 1992; 68:869–877. [PubMed: 1547488]
35. Hao Z, Rajewsky K. Homeostasis of Peripheral B Cells in the Absence of B Cell Influx from the Bone Marrow. J. Exp. Med. 2001; 194:1151–1164. [PubMed: 11602643]

36. Coster G, Gold A, Chen D, Schatz DG, Goldberg M. A Dual Interaction between the DNA Damage Response Protein MDC1 and the RAG1 Subunit of the V(D)J Recombinase. J. Biol. Chem. 2012; 287:36488–36498. [PubMed: 22942284]
37. Bredemeyer AL, Sharma C-Y, Huang GG, Helmink BA, Walker LM, Khor KC, Nuskey B, Sullivan KE, Pandita TK, Bassing CH, Sleckman BP. ATM stabilizes DNA double-strand-break complexes during V(D)J recombination. Nature. 2006; 442:466–470. [PubMed: 16799570]
38. Savic V, Yin B, Maas NL, Bredemeyer AL, Carpenter AC, Helmink BA, Yang-Iott KS, Sleckman BP, Bassing CH. Formation of Dynamic γ-H2AX Domains along Broken DNA Strands Is Distinctly Regulated by ATM and MDC1 and Dependent upon H2AX Densities in Chromatin. Mol. Cell. 2009; 34:298–310. [PubMed: 19450528]
39. Gapud EJ, Lee B-S, Mahowald GK, Bassing CH, Sleckman BP. Repair of Chromosomal RAG-Mediated DNA Breaks by Mutant RAG Proteins Lacking Phosphatidylinositol 3-Like Kinase Consensus Phosphorylation Sites. J. Immunol. 2011; 187:1826–1834. [PubMed: 21742970]
40. Yin B, Savic V, Juntilla MM, Bredemeyer AL, Yang-Iott KS, Helmink BA, Koretzky GA, Sleckman BP, Bassing CH. Histone H2AX stabilizes broken DNA strands to suppress chromosome breaks and translocations during V(D)J recombination. J. Exp. Med. 2009; 206:2625–2639. [PubMed: 19887394]
41. DeMicco A, Reich T, Arya R, Rivera-Reyes A, Fisher MR, Bassing CH. Lymphocyte Lineage-Specific and Developmental Stage Specific Mechanisms Suppress Cyclin D3 Expression in Response to DNA Double Strand Breaks. Cell Cycle Georget. Tex. 2016 0.
42. Rolink A, Grawunder U, Haasner D, Strasser A, Melchers F. Immature surface Ig+ B cells can continue to rearrange kappa and lambda L chain gene loci. J. Exp. Med. 1993; 178:1263–1270. [PubMed: 8376934]
43. Billips LG, Nuñez CA, Bertrand FE, Stankovic AK, Gartland GL, Burrows PD, Cooper MD. Immunoglobulin recombinase gene activity is modulated reciprocally by interleukin 7 and CD19 in B cell progenitors. J. Exp. Med. 1995; 182:973–982. [PubMed: 7561700]
44. Hecht SM. Bleomycin: new perspectives on the mechanism of action. J. Nat. Prod. 2000; 63:158–168. [PubMed: 10650103]
45. Montecucco A, Zanetta F, Biamonti G. Molecular mechanisms of etoposide. EXCLI J. 2015; 14:95–108. [PubMed: 26600742]
46. Rodgers W, Byrum JN, Sapkota H, Rahman NS, Cail RC, Zhao S, Schatz DG, Rodgers KK. Spatio-temporal regulation of RAG2 following genotoxic stress. DNA Repair. 2015; 27:19–27. [PubMed: 25625798]
47. Grawunder U, Schatz DG, Leu TM, Rolink A, Melchers F. The half-life of RAG-1 protein in precursor B cells is increased in the absence of RAG-2 expression. J. Exp. Med. 1996; 183:1731–1737. [PubMed: 8666930]
48. Lin WC, Desiderio S. Regulation of V(D)J recombination activator protein RAG-2 by phosphorylation. Science. 1993; 260:953–959. [PubMed: 8493533]
49. McBlane JF, van Gent DC, Ramsden DA, Romeo C, Cuomo CA, Gellert M, Oettinger MA. Cleavage at a V(D)J recombination signal requires only RAG1 and RAG2 proteins and occurs in two steps. Cell. 1995; 83:387–395. [PubMed: 8521468]
50. Lin W-C, Desiderio S. Cell cycle regulation of V (D) J recombination-activating protein RAG-2. Proc. Natl. Acad. Sci. 1994; 91:2733–2737. [PubMed: 8146183]
51. Li Z, Dordai DI, Lee J, Desiderio S. A conserved degradation signal regulates RAG-2 accumulation during cell division and links V (D) J recombination to the cell cycle. Immunity. 1996; 5:575–589. [PubMed: 8986717]
52. Hann SR, Eisenman RN. Proteins encoded by the human c-myc oncogene: differential expression in neoplastic cells. Mol. Cell. Biol. 1984; 4:2486–2497. [PubMed: 6513926]
53. Verkoczy L, Aït-Azzouzene D, Skog P, Märtensson A, Lang J, Duong B, Nemazee D. A Role for Nuclear Factor Kappa B/Rel Transcription Factors in the Regulation of the Recombinase Activator Genes. Immunity. 2005; 22:519–531. [PubMed: 15845455]
54. Barlow C, Brown KD, Deng CX, Tagle DA, Wynshaw-Boris A. Atm selectively regulates distinct p53-dependent cell-cycle checkpoint and apoptotic pathways. Nat. Genet. 1997; 17:453–456. [PubMed: 9398849]

55. Muljo SA, Schlissel MS. A small molecule Abl kinase inhibitor induces differentiation of Abelson virus−transformed pre-B cell lines. Nat. Immunol. 2003; 4:31–37. [PubMed: 12469118]
56. Moshous D, Callebaut I, de Chasseval R, Corneo B, Cavazzana-Calvo M, Le Deist F, Tezcan I, Sanal O, Bertrand Y, Philippe N, Fischer A, de Villartay JP. Artemis, a novel DNA double-strand break repair/V(D)J recombination protein, is mutated in human severe combined immune deficiency. Cell. 2001; 105:177–186. [PubMed: 11336668]
57. Hewitt SL, Yin B, Ji Y, Chaumeil J, Marszalek K, Tenthorey J, Salvagiotto G, Steinel N, Ramsey LB, Ghysdael J, Farrar MA, Sleckman BP, Schatz DG, Busslinger M, Bassing CH, Skok JA. RAG-1 and ATM coordinate monoallelic recombination and nuclear positioning of immunoglobulin loci. Nat. Immunol. 2009; 10:655–664. [PubMed: 19448632]
58. Liang H-E, Hsu L-Y, Cado D, Cowell LG, Kelsoe G, Schlissel MS. The “dispensable” portion of RAG2 is necessary for efficient V-to-DJ rearrangement during B and T cell development. Immunity. 2002; 17:639–651. [PubMed: 12433370]
59. Zhang Y-H, Shetty K, Surleac MD, Petrescu AJ, Schatz DG. Mapping and Quantitation of the Interaction between the Recombination Activating Gene Proteins RAG1 and RAG2. J. Biol. Chem. 2015; 290:11802–11817. [PubMed: 25745109]
60. Chan EAW, Teng G, Corbett E, Choudhury KR, Bassing CH, Schatz DG, Krangel MS. Peripheral subnuclear positioning suppresses Tcrb recombination and segregates Tcrb alleles from RAG2. Proc. Natl. Acad. Sci. 2013; 110:E4628–E4637. [PubMed: 24218622]
61. Rothkamm K, Löbrich M. Evidence for a lack of DNA double-strand break repair in human cells exposed to very low x-ray doses. Proc. Natl. Acad. Sci. U. S. A. 2003; 100:5057–5062. [PubMed: 12679524]
62. Muslimović A, Nyström S, Gao Y, Hammarsten O. Numerical analysis of etoposide induced DNA breaks. PloS One. 2009; 4:e5859. [PubMed: 19516899]
63. Hayden MS, Ghosh S. NF-κB, the first quarter-century: remarkable progress and outstanding questions. Genes Dev. 2012; 26:203–234. [PubMed: 22302935]
64. Smale ST. Dimer-specific regulatory mechanisms within the NF-κB family of transcription factors. Immunol. Rev. 2012; 246:193–204. [PubMed: 22435556]
65. Smale ST. Hierarchies of NF-κB target-gene regulation. Nat. Immunol. 2011; 12:689–694. [PubMed: 21772277]
66. Tong X, Yin L, Washington R, Rosenberg DW, Giardina C. The p50-p50 NF-kappaB complex as a stimulus-specific repressor of gene activation. Mol. Cell. Biochem. 2004; 265:171–183. [PubMed: 15543947]
67. Bohuslav J, Kravchenko VV, Parry GC, Erlich JH, Gerondakis S, Mackman N, Ulevitch RJ. Regulation of an essential innate immune response by the p50 subunit of NF-kappaB. J. Clin. Invest. 1998; 102:1645–1652. [PubMed: 9802878]
68. Scherer DC, Brockman JA, Bendall HH, Zhang GM, Ballard DW, Oltz EM. Corepression of RelA and c-rel inhibits immunoglobulin kappa gene transcription and rearrangement in precursor B lymphocytes. Immunity. 1996; 5:563–574. [PubMed: 8986716]
69. Ochodnicka-Mackovicova K, Bahjat M, Bloedjes TA, Maas C, de Bruin AM, Bende RJ, van Noesel CJM, Guikema JEJ. NF- B and AKT signaling prevent DNA damage in transformed pre-B cells by suppressing RAG1/2 expression and activity. Blood. 2015; 126:1324–1335. [PubMed: 26153519]
70. Verma UN. Nuclear Role of I B Kinase- /NF- B Essential Modulator (IKK /NEMO) in NF- B-dependent Gene Expression. J. Biol. Chem. 2003; 279:3509–3515. [PubMed: 14597638]
71. Yang Y, Xia F, Hermance N, Mabb A, Simonson S, Morrissey S, Gandhi P, Munson M, Miyamoto S, Kelliher MA. A cytosolic ATM/NEMO/RIP1 complex recruits TAK1 to mediate the NF-kappaB and p38 mitogen-activated protein kinase (MAPK)/MAPK-activated protein 2 responses to DNA damage. Mol. Cell. Biol. 2011; 31:2774–2786. [PubMed: 21606198]
72. Yannoutsos N, Barreto V, Misulovin Z, Gazumyan A, Yu W, Rajewsky N, Peixoto BR, Eisenreich T, Nussenzweig MC. A cis element in the recombination activating gene locus regulates gene expression by counteracting a distant silencer. Nat. Immunol. 2004; 5:443–450. [PubMed: 15021880]

73. Brady BL, Steinel NC, Bassing CH. Antigen Receptor Allelic Exclusion: An Update and Reappraisal. J. Immunol. 2010; 185:3801–3808. [PubMed: 20858891]

74. Mostoslavsky R, Singh N, Tenzen T, Goldmit M, Gabay C, Elizur S, Qi P, Reubinoff BE, Chess A, Cedar H, Bergman Y. Asynchronous replication and allelic exclusion in the immune system. Nature. 2001; 414:221–225. [PubMed: 11700561]

75. Schlimgen RJ, Reddy KL, Singh H, Krangel MS. Initiation of allelic exclusion by stochastic interaction of Tcrb alleles with repressive nuclear compartments. Nat. Immunol. 2008; 9:802–809. [PubMed: 18536719]

76. Skok JA, Gisler R, Novatchkova M, Farmer D, de Laat W, Busslinger M. Reversible contraction by looping of the Tcra and Tcrb loci in rearranging thymocytes. Nat. Immunol. 2007; 8:378–387. [PubMed: 17334367]

77. Hah Y-S, Lee JH, Kim DR. DNA-dependent protein kinase mediates V(D)J recombination via RAG2 phosphorylation. J. Biochem. Mol. Biol. 2007; 40:432–438. [PubMed: 17562296]

78. Lin JM, Landree MA, Roth DB. V (D) J recombination catalyzed by mutant RAG proteins lacking consensus DNA-PK phosphorylation sites. Mol. Immunol. 1999; 36:1263–1269. [PubMed: 10684966]

79. Um J-H, Brown AL, Singh SK, Chen Y, Gucek B-S, Lee M, Luckey MA, Kim J-H, Park MK, Sleckman BP, Gellert M, Chung JH. Metabolic sensor AMPK directly phosphorylates RAG1 protein and regulates V(D)J recombination. Proc. Natl. Acad. Sci. 2013; 110:9873–9878. [PubMed: 23716691]

80. Richardson C, Jasin M. Frequent chromosomal translocations induced by DNA double-strand breaks. Nature. 2000; 405:697–700. [PubMed: 10864328]

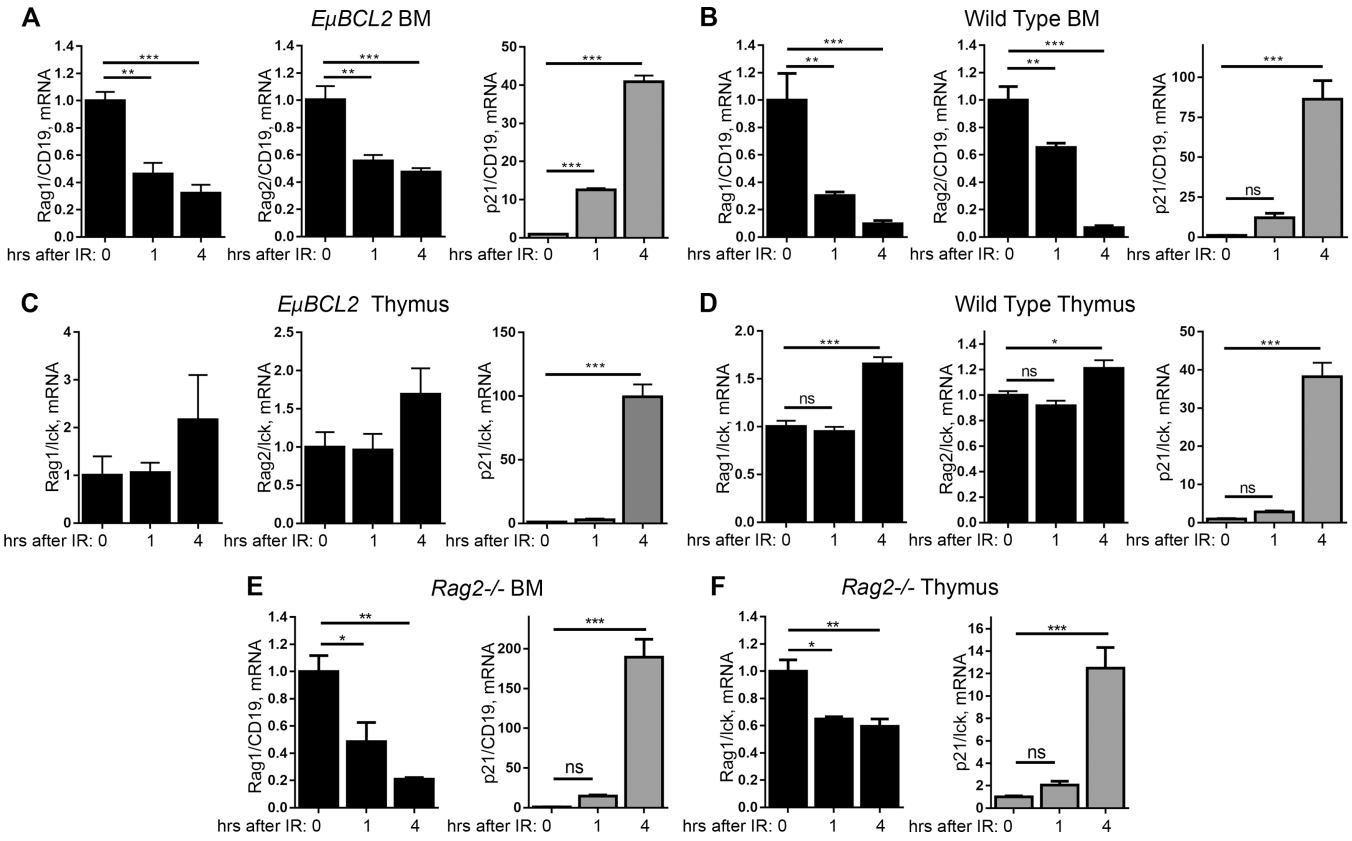

FIGURE 1.

Immature B and T lymphocytes suppress *Rag1* and *Rag2* expression in response to ionizing radiation. (**A**) qRT-PCR quantification of Rag1, Rag2, and p21 mRNA in BM from non-irradiated *EμBCL2* mice or *EμBCL2* mice at indicated times after exposure to 10 Gy IR. Data are from one experiment with 3–4 mice for each timepoint. (**B**) qRT-PCR quantification of Rag1, Rag2, and p21 mRNA in thymuses from non-irradiated *EμBCL2* mice or *EμBCL2* mice at indicated times after exposure to 10 Gy IR. Data are from three independent experiments including a total of 3–6 mice per timepoint. (**C**) qRT-PCR quantification of Rag1, Rag2, and p21 mRNA in BM from non-irradiated wild-type mice at indicated times after exposure to 10 Gy IR. Data are from two independent experiments including a total of 4–5 mice per timepoint. (**D**) qRT-PCR quantification of Rag1, Rag2, and p21 mRNA in thymus from non-irradiated wild-type mice or wild-type mice at indicated times after exposure to 10 Gy IR. Data are from two independent experiments including a total of 4–5 mice per timepoint. (**E**) qRT-PCR quantification of Rag1 and p21 mRNA in BM from non-irradiated *Rag2*$^{-/-}$ mice or *Rag2*$^{-/-}$ mice at indicated times after exposure to 10 Gy IR. Data are from one experiment with 3 or 4 mice per timepoint. (**F**) qRT-PCR quantification of Rag1 and p21 mRNA in thymus from non-irradiated *Rag2*$^{-/-}$ mice or *Rag2*$^{-/-}$ mice at indicated times after exposure to 10 Gy IR. Data are from one experiment with 3 or 4 mice per timepoint. (**A–F**) Data averages are shown with error bars indicating SEM. p-values calculated using Dunnett's post-test after ANOVA. *p<0.05, **p<0.01, ***p<0.001.

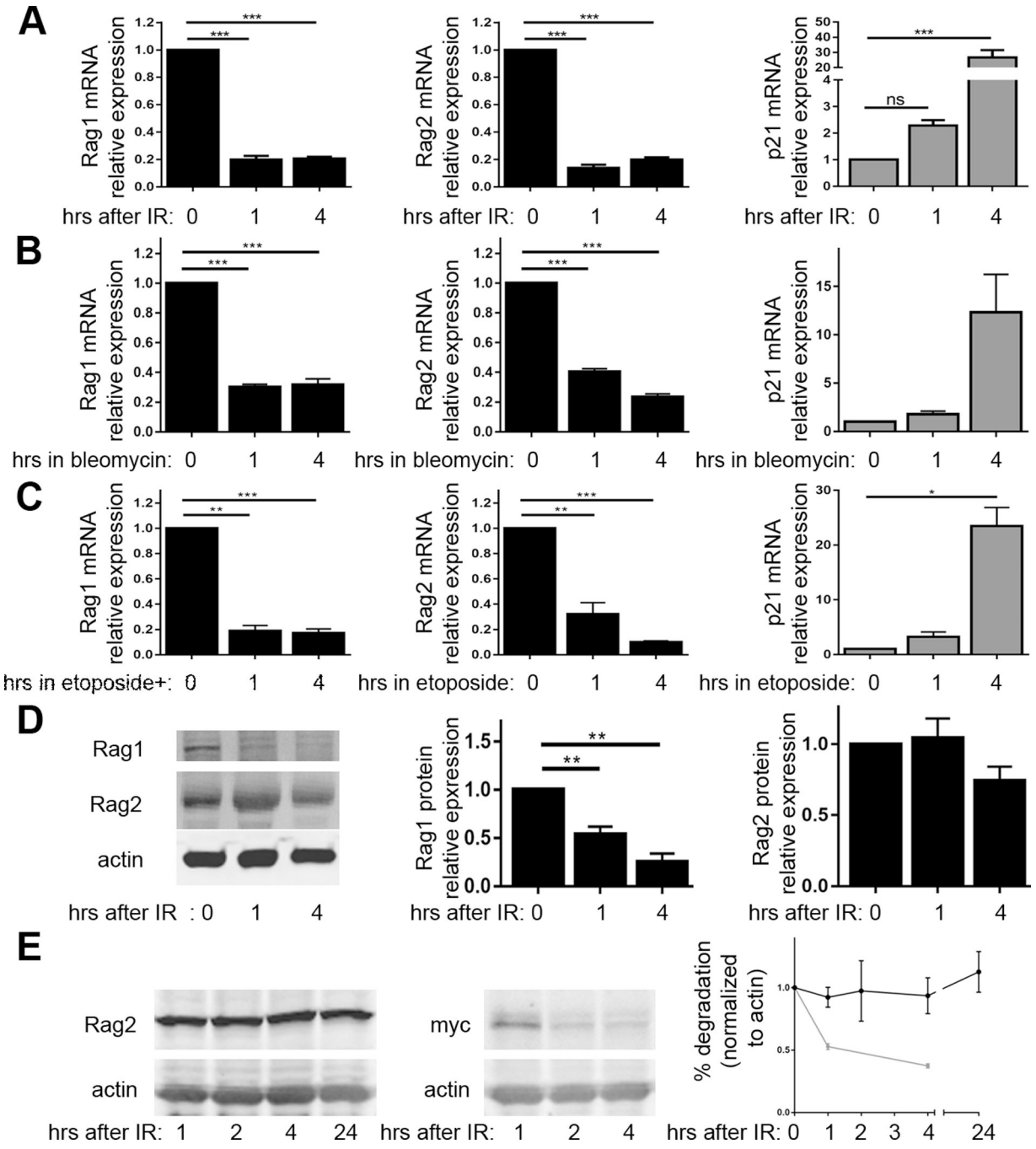

FIGURE 2.

DSBs induced in pre-B cells suppress downregulate Rag1 and Rag2 mRNA and Rag1 protein. (**A**) qRT-PCR quantification of Rag1, Rag2, and p21 mRNA in non-irradiated *EμBCL2* pre-B cells or irradiated *EμBCL2* pre-B cells at indicated times after exposure to 4 Gy IR. Data are from 11 independent experiments. (**B**) qRT-PCR quantification of Rag1, Rag2, and p21 mRNA in *EμBCL2* pre-B cells or *EμBCL2* pre-B cells at indicated times after addition of 5 μM bleomycin to culture media. Data are from 3 independent experiments. (**C**) qRT-PCR quantification of Rag1, Rag2, and p21 mRNA in *EμBCL2* pre-B

cells or *EμBCL2* pre-B cells at indicated times after addition of 10 mg/mL etoposide to culture media. Data are from 3 independent experiments. (**D**) Representative western blot analysis and graphs depicting quantification of Rag1 and Rag2 protein in non-irradiated *EμBCL2* pre-B cells or irradiated *EμBCL2* pre-B cells at indicated times after exposure to 4 Gy IR. Data are from 8 independent experiments. (**E**) Representative western blot analysis and graphs depicting quantification of Rag2 and c-Myc protein in cycloheximide-treated non-irradiated *EμBCL2* pre-B cells or irradiated *EμBCL2* pre-B cells at indicated times after exposure to 4 Gy IR. Data are from 3 independent experiments. (**A–E**) Data are normalized to 1.0 for non-irradiated cells within each experiment. For irradiated cells, data averages are shown with error bars indicating SEM. p-values calculated using Dunnett's post-test after ANOVA. **p<0.01, ***p<0.001.

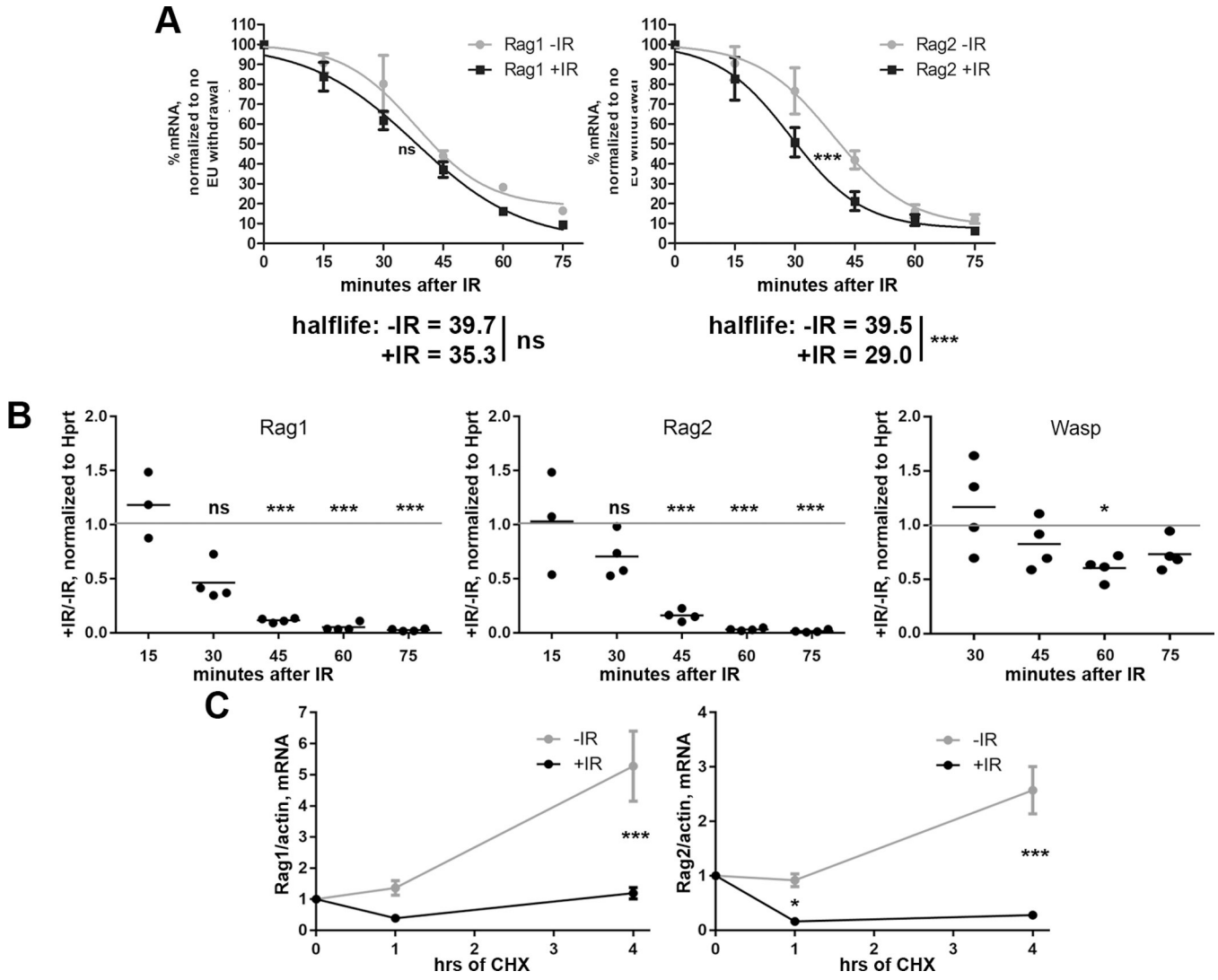

FIGURE 3.

DSBs induced in primary pre-B cells immediately repress *Rag1* and *Rag2* transcription. (**A**) qRT-PCR quantification of EU-labeled Rag1 and Rag2 mRNA levels relative to EU-labeled 18S RNA levels in non-irradiated *EμBCL2* pre-B cells or irradiated *EμBCL2* pre-B cells at indicated times after EU washout and/or exposure to 4 Gy of IR. Data are from 4 independent experiments. Data averages are shown with error bars the SEM. Prism 5 was used to calculate best-fit curves, half-lives and p-values. ***p<0.001. (**B**) qRT-PCR quantification of EU-labeled Rag1, Rag2, and Wasp mRNA levels relative to EU-labeled Hprt mRNA levels in non-irradiated *EμBCL2* pre-B cells and irradiated *EμBCL2* pre-B cells at indicated times after addition of EU and exposure to 4 Gy of IR. Data are presented as the ratio of relative levels of each mRNA in irradiated cells compared to non-irradiated cells. The dotted line represents a value of 1, which would indicate that IR had no effect on the transcription rate of a gene. Data are from 4 independent experiments. p-values for whether the average ratio at each time point is different from 1.0 was determined using one-tailed T test with Bonferroni's correction for multiple testing. ***p<0.001. (**C**) qRT-PCR

quantification of Rag1 and Rag2 mRNA in cycloheximide-treated non-irradiated *EμBCL2* pre-B cells or irradiated *EμBCL2* pre-B cells at indicated times after exposure to 4 Gy IR. Data are from 3 independent experiments. Data averages are shown with error bars the SEM. p-values were calculated by T test with Bonferroni's correction for multiple testing. ***p<0.001.

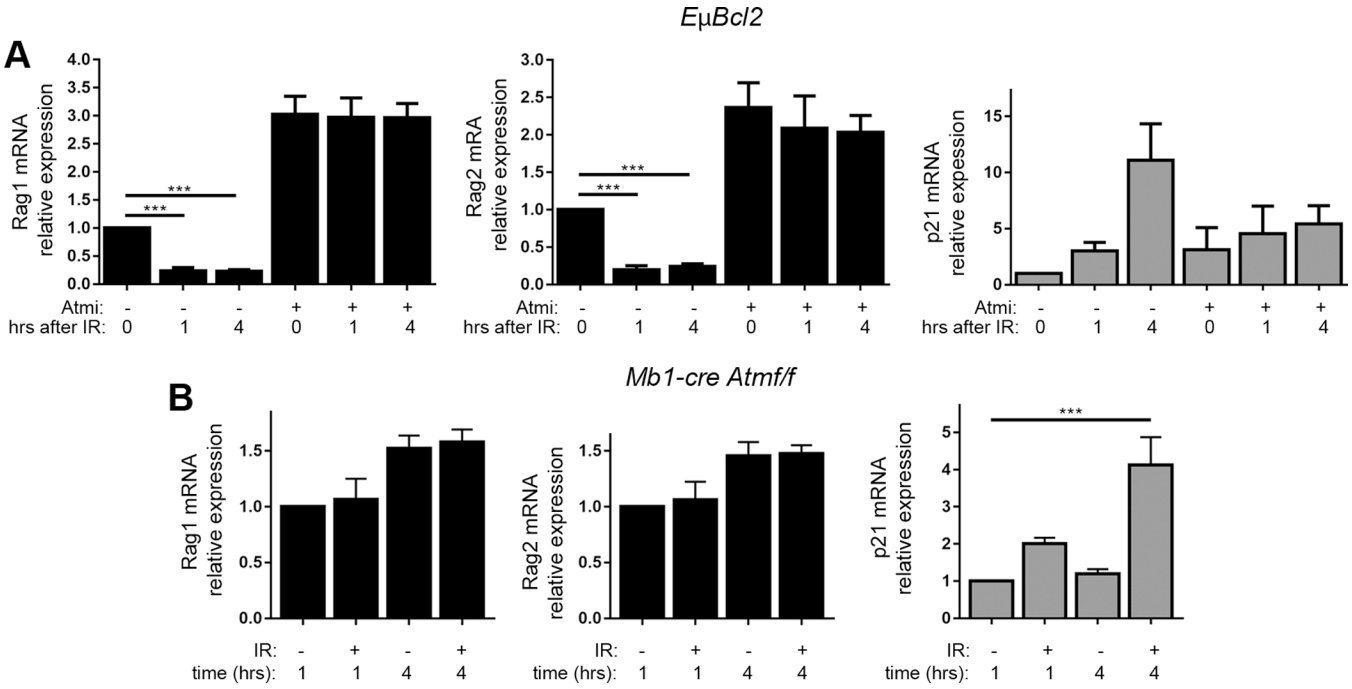

FIGURE 4.

ATM and Nemo are required for DSBs induced in pre-B cells to downregulate *Rag1* and *Rag2* expression. (**A**) qRT-PCR quantification of Rag1, Rag2, and p21 mRNA in non-irradiated *EμBCL2* pre-B cells or irradiated *EμBCL2* pre-B cells at indicated times after exposure to 4 Gy of IR. Cells were treated with 15 μM of the KU55933 ATM kinase inhibitor or vehicle (DMSO) for 48 hours prior to irradiation or harvesting of non-irradiated cells. Data are from 8 independent experiments. Data are normalized to 1.0 for non-irradiated, vehicle-treated cells within each experiment. For other conditions, data averages are shown with error bars indicating SEM. p-values were calculated by Dunnett's post-test after ANOVA. ***p<0.001. (**B**) qRT-PCR quantification of Rag1, Rag2, and p21 mRNA in non-irradiated *Mb1Cre*$^{+}$*Atm*$^{flox/flox}$ pre-B cells or irradiated *Mb1Cre*$^{+}$*Atm*$^{flox/flox}$ pre-B cells at indicated times after exposure to 4 Gy IR. Data are from 3 independent experiments. Data are normalized to 1.0 for non-irradiated cells harvested one hour following IR exposure of irradiated samples. For other samples, data averages are shown with error bars indicating SEM. p-values were calculated by Dunnett's post-test after ANOVA. ***p<0.001.

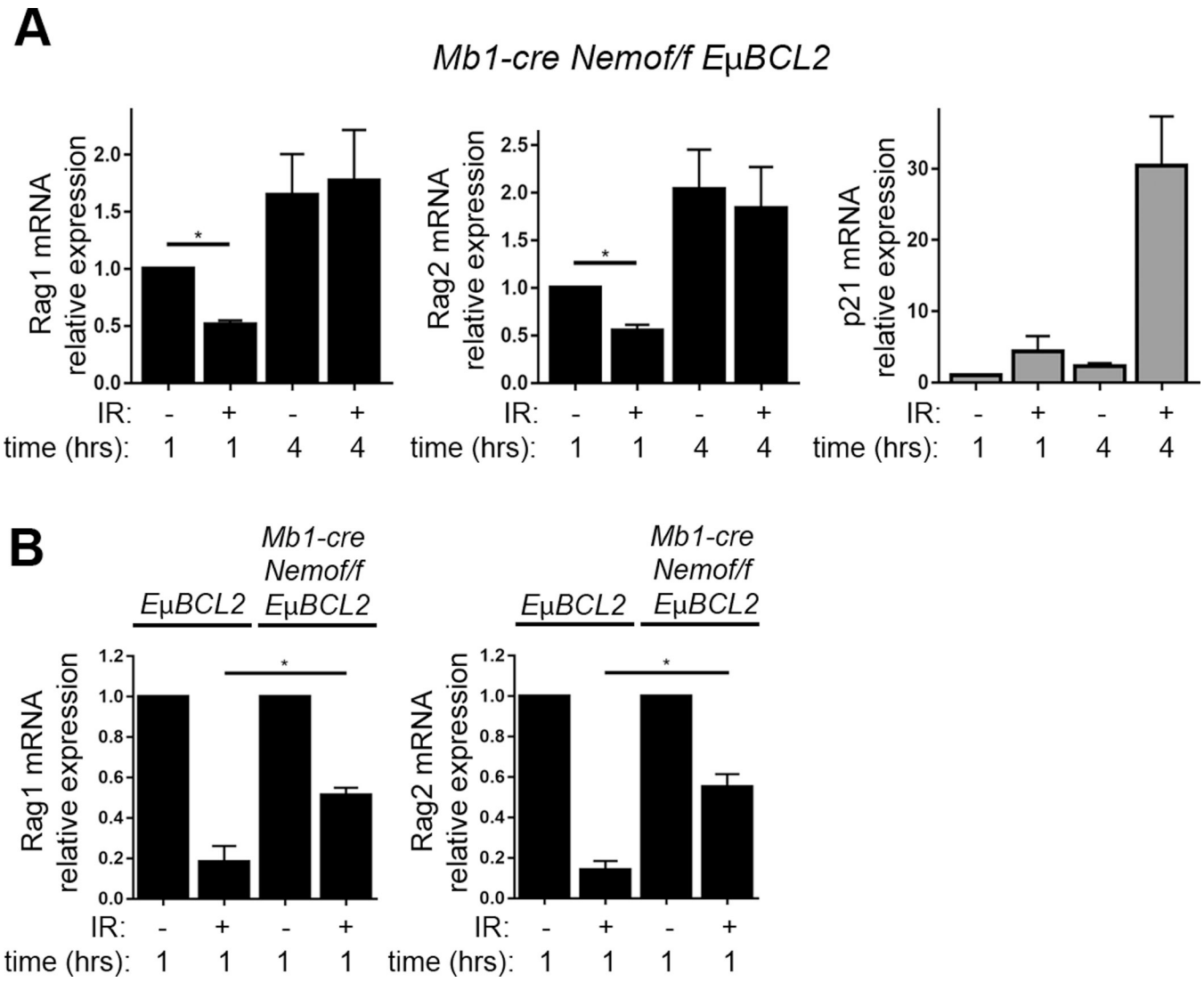

FIGURE 5.

Nemo is required for pre-B cells to normally downregulate *Rag1* and *Rag2* expression in response to DSBs. (**A**) qRT-PCR quantification of Rag1, Rag2, and p21 mRNA in non-irradiated *Mb1Cre*$^{+}$*Nemo*$^{flox/flox}$*EμBCL2* pre-B cells or irradiated *Mb1Cre*$^{+}$*Nemo*$^{flox/flox}$*EμBCL2* pre-B cells at indicated times after exposure to 4 Gy IR. Data are from 3 independent experiments. p-values were calculated by Dunnett's post-test after ANOVA. *p<0.05. (**B**) qRT-PCR quantification of Rag1 and Rag2 mRNA in non-irradiated or irradiated pre-B cells from *EμBCL2* or *Mb1Cre*$^{+}$*Nemo*$^{flox/flox}$*EμBCL2* mice at 1 hour after exposure to 4 Gy IR. Data are from 3 independent experiments. p-value was calculated by T test. *p<0.05. (**A**–**B**) Data are normalized to 1.0 for non-irradiated cells harvested one hour following IR exposure of irradiated samples. For other samples, data averages are shown with error bars indicating SEM.

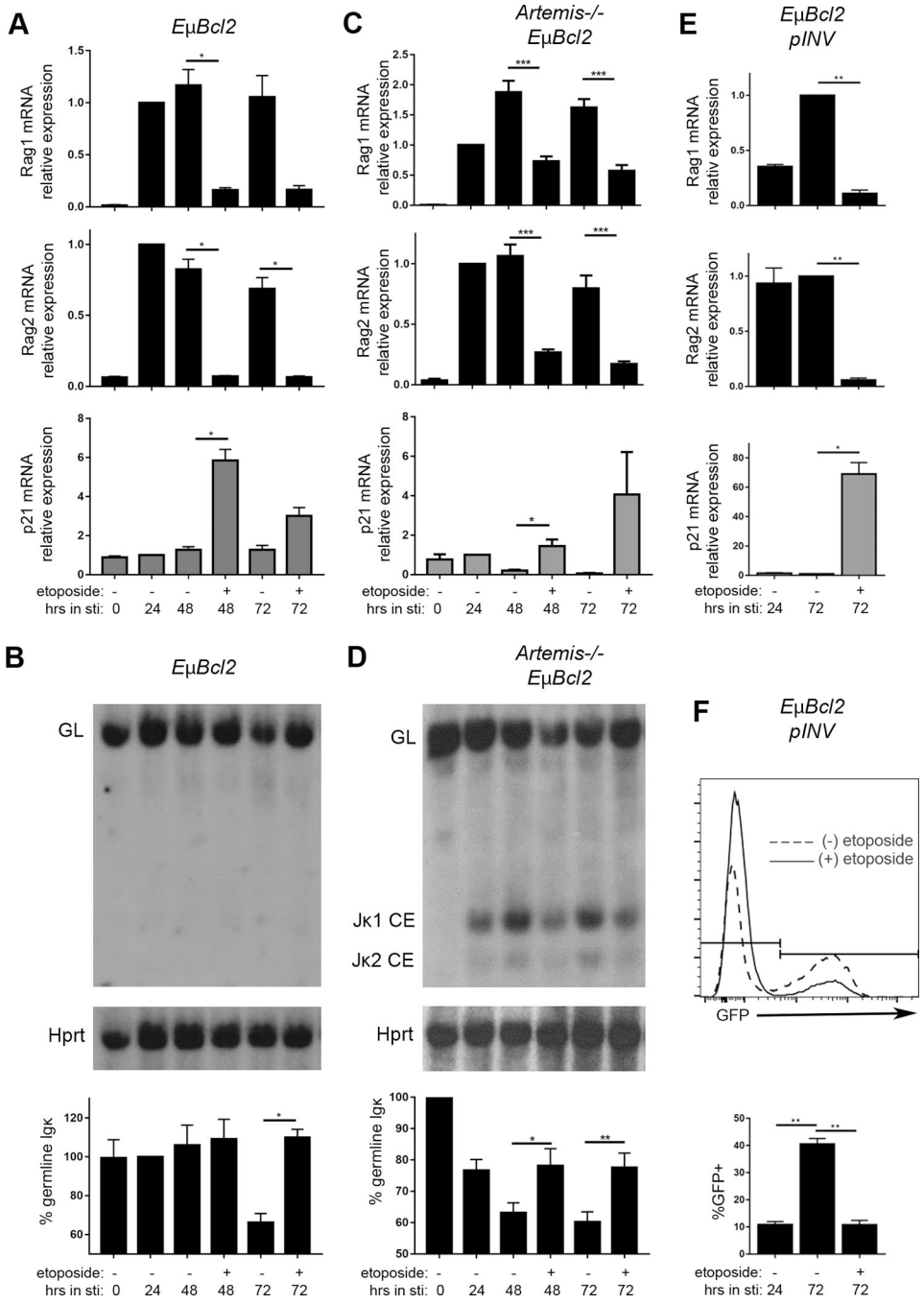

FIGURE 6.

Etoposide inhibits recombination of endogenous *Igκ* loci and an integrated substrate. (**A**) qRT-PCR quantification of Rag1, Rag2, and p21 mRNA in *EμBCL2* Abl cells untreated or treated with STI571 or STI571 and etoposide for the indicated amounts of time. Data are from 3 independent experiments. (**B**) Representative Southern analysis and graphical quantification of *Igκ* recombination in *EμBCL2* Abl cells untreated or treated with STI571 or STI571 and etoposide for the indicated amounts of time. Data are from 3 independent experiments. (**C**) qRT-PCR quantification of Rag1, Rag2, and p21 mRNA in

Artemis$^{-/-}$*EμBCL2* Abl cells untreated or treated with STI571 or STI571 and etoposide for the indicated amounts of time. Data are from 6 independent experiments. (**D**) Representative Southern blot analysis and graphical quantification of *Jκ* cleavage in *Artemis*$^{-/-}$*EμBCL2* Abl cells untreated or treated with STI571 or STI571 and etoposide for the indicated amounts of time. Data are from 6 independent experiments. (**E**) qRT-PCR quantification of Rag1, Rag2, and p21 mRNA in *EμBCL2-pINV* Abl cells treated with STI571 or STI571 and etoposide for the indicated amounts of time. Data are from 3 independent experiments. (**F**) Representative flow cytometric analysis and graphical quantification of *pINV* recombination in *EμBCL2-pINV* Abl cells treated with STI571 or STI571 and etoposide for the indicated amounts of time. Data are from 4 independent experiments. (**A–F**) Data averages are shown with error bars the SEM. p-values were determined by Dunnett's post-test after ANOVA. *p<0.05, **p<0.01, ***p<0.001.